ARTICLES
https://doi.org/10.1038/s41564-021-00922-y

nature microbiology

Transcription in fungal conidia before dormancy produces phenotypically variable conidia that maximize survival in different environments

Fang Wang[1], Pooja Sethiya[1], Xiaohui Hu[1,2], Shuhui Guo[1], Yingying Chen[1], Ang Li[1], Kaeling Tan[1,3] and Koon Ho Wong[1,4,5] ✉

Fungi produce millions of clonal asexual conidia (spores) that remain dormant until favourable conditions occur. Conidia contain abundant stable messenger RNAs but the mechanisms underlying the production of these transcripts and their composition and functions are unknown. Here, we report that the conidia of three filamentous fungal species (*Aspergillus nidulans*, *Aspergillus fumigatus*, *Talaromyces marneffei*) are transcriptionally active and can synthesize mRNAs. We find that transcription in fully developed conidia is modulated in response to changes in the environment until conidia leave the developmental structure. Environment-specific transcriptional responses can alter conidial content (mRNAs, proteins and secondary metabolites) and change gene expression when dormancy is broken. Conidial transcription affects the fitness and capabilities of fungal cells after germination, including stress and antifungal drug (azole) resistance, mycotoxin and secondary metabolite production and virulence. The transcriptional variation that we characterize in fungal conidia explains how genetically identical conidia mature into phenotypically variable conidia. We find that fungal conidia prepare for the future by synthesizing and storing transcripts according to environmental conditions present before dormancy.

In the model organism *Aspergillus nidulans*, the asexual reproductive process (known as conidiation) involves the formation of a conidiophore beginning with the emergence and extension of a stalk from a specialized foot cell of vegetative hyphae. The tip of the stalk then swells to form a vesicle where the sterigmata (metulae and phialides) develop. Chains of individual conidia sequentially bud from the phialides, giving rise to thousands of conidia per conidiophore. Fully developed conidia may leave the developmental structure at any time and can remain dormant for long periods until they encounter favourable conditions[1,2] under which they germinate to initiate a new life cycle. Dormancy of fungal conidia is rather ill defined, broadly referring to the resting state of fully developed, viable conidia before germination. However, this so-called dormant state may be due to different factors, such as an active block in germination, senescence or simply cellular inactivity resulting from low intracellular water content. How fungal conidia establish dormancy is not clear.

Studies in different fungi have shown that genetically identical spores formed under different environmental conditions or of different developmental ages possess distinct physical and physiological properties[3–21]. Recent single-cell studies on *Aspergillus fumigatus* conidia indicated that conidia heterogeneity is not due to genetic inheritance but rather to an intrinsic factor (or factors) yet to be identified[6,16]. Phenotypic heterogeneity in heat tolerance and susceptibility to macrophage phagocytosis has been associated with specific protein and chemical contents in spores[4,8,13,22]; these observations imply gene expression variation, which is also a basis for mycelium heterogeneity[23] and microbial phenotypic heterogeneity[24–26] among conidia. The molecular mechanisms underlying the gene expression differences between conidia are not known.

Fungal conidia contain large amounts of highly stable transcripts[1,21,27–34]. The purpose of these transcripts is controversial. While some reports have suggested that conidial transcripts prime conidia for gene expression when dormancy is broken[1,29,34], others have suggested that they are merely remnants from the conidial developmental process[28]. Considering that conidia have no[2,34,35] or very low[29,36] metabolic activity, how conidial transcripts originate is also an intriguing question. It is generally believed that conidial transcripts are initially synthesized in the conidiophore structure and packaged into individual conidia during development; however, this has never been experimentally proven.

Results

The so-called dormant fungal conidia are transcriptionally active. To determine whether fungal conidia have transcription activity to synthesize their own transcripts during development, we applied chromatin immunoprecipitation followed by sequencing (ChIP–seq) to map the genome-wide occupancy of elongating RNA polymerase II (RNAP II) in conidia of *A. nidulans* and two pathogenic fungi, *A. fumigatus* and *Talaromyces marneffei*. Formaldehyde cross-linking was carried out directly on culture plates before collecting the conidia to study the condition where conidia are still attached to the developmental structure conidiophores. Surprisingly, RNAP II ChIP–seq signals were found for approximately 1,000 genes in each species (Fig. 1a and Extended Data Fig. 1a,b) and a similar number was detected in actively growing hyphae (Supplementary Table 1). Those genes were enriched in similar physiological functions among the three species (Extended Data Fig. 1c and Supplementary Table 2). In the case of *A. nidulans*,

[1]Faculty of Health Sciences, University of Macau, Macau SAR, China. [2]Drug Development Core, Faculty of Health Sciences, University of Macau, Macau SAR, China. [3]Genomics, Bioinformatics and Single Cell Analysis Core, Faculty of Health Sciences, University of Macau, Macau SAR, China. [4]Institute of Translational Medicine, Faculty of Health Sciences, University of Macau, Macau SAR, China. [5]MoE Frontiers Science Center for Precision Oncology, University of Macau, Macau SAR, China. ✉e-mail: koonhowong@um.edu.mo

a high RNAP II occupancy was observed on known conidia-specific genes[37–39] (Extended Data Fig. 1d) but not on genes required for conidia formation[40] (that is, known regulators of conidiation) (Extended Data Fig. 1e) or those with hyphae-specific functions[41,42] (Extended Data Fig. 1f). Importantly, microscopic analysis showed that the conidia preparations were free of contaminating hyphal cells (Extended Data Fig. 1g), confirming that the observed RNAP II bindings were indeed conidia-specific.

The RNAP II signals may reflect either active transcription or non-productive RNAP II binding. In *Saccharomyces cerevisiae*, the levels of transcription initiation and transcription elongation are correlated to active transcriptional events[43]. ChIP–seq against the preinitiation complex (TATA box-binding protein-like 1 (TBP)^{MYC} and transcription initiation factor IIB (TFIIB)^{MYC}) showed a positive correlation between the two processes in *A. nidulans* conidia (Fig. 1b–d); the correlation is similar to that of actively growing hyphae (Fig. 1e), which have active and productive transcriptional activities. Furthermore, as expected for active transcription, promoter nucleosome depletion (as measured by histone H3 occupancy) and histone modifications associated with active transcription (for example, H3 acetylation (H3Ac), H3 lysine 4 trimethylation (H3K4me3) and H3 lysine 36 trimethylation (H3K36me3)) were also found for genes with a strong RNAP II occupancy (Fig. 1f,g). Most importantly, these genes had high messenger RNA levels and there was a good correlation between overall RNAP II occupancy and mRNA levels (Fig. 1h). These results demonstrated that conidia have robust transcription activity for mRNA synthesis while still attached to their conidiophores.

We next focused on *A. nidulans* and determined whether RNA polymerase I (RNAP I) and RNA polymerase III (RNAP III) transcriptions are also active in conidia for ribosomal RNA and transfer RNA synthesis, respectively. ChIP–seq showed that conidia also have active RNAP I and RNAP III transcriptional activities (Fig. 1i,j). Notably, both RNAP I and RNAP III transcription levels were significantly lower in conidia than in hyphae (Extended Data Fig. 1h,i), in contrast to the situation observed for RNAP II transcription (Extended Data Fig. 1j). This result may reflect a difference in the relative levels of the translation apparatus and mRNAs between conidia and hyphae. It is noteworthy that the RNAP II-transcribed ribosomal protein genes, which encode the protein constituents of the translation machinery, were actually expressed at comparable levels between conidia and hyphae (Extended Data Fig. 1k). Since conidia are not actively growing, have limited cellular resources and probably require relatively less (or no) protein synthesis, lowering RNAP I and RNAP III transcription may serve both regulatory and conservation purposes. Taken together, we demonstrated that all three RNA polymerases present robust transcriptional activity in filamentous fungal conidia and can, therefore, synthesize their own transcripts. This finding challenges the prevailing belief that conidial transcripts are synthesized in the conidiophores and then packaged into individual conidia during development.

Conidia on conidiophores are transcriptionally responsive to the environment. Environmental conditions can influence conidia development. It is generally assumed that environmental cues are sensed and responded to by hyphae and developmental cells. We found that conidia on conidiophores could also produce a heat-shock transcriptional response (Extended Data Fig. 2a,b) similar to proliferating hyphal cells (Extended Data Fig. 2c). Strikingly, at the genome-wide level, dramatic transcriptional remodelling occurred in *A. nidulans* conidia after exposure to temperature shocks (4 or 42 °C, referred to as cold-shocked or heat-shocked conidia, respectively) (Fig. 2a,b) or when the conidia formed under different growth conditions such as zinc deficiency (referred to as zinc-starved conidia) or high osmolarity (0.5 M of NaCl or 0.5 M of KCl, referred to as NaCl or KCl conidia, respectively) (Fig. 2c,d). On average, several hundred genes were differentially induced under each defined condition (Supplementary Table 3) and were enriched for physiologically relevant factors such as heat-shock proteins for heat shock (Fig. 2e), sphingolipids for cold treatment (Extended Data Fig. 2d), the transcriptional regulator of zinc homeostasis ZapA[44] and zinc ion transporters for zinc-limited conditions (Fig. 2f) and glycerol transporters for conditions of high osmolarity (Fig. 2g and Extended Data Fig. 2e), as well as many others (Extended Data Fig. 2d and Supplementary Table 4). Similar results were observed for the human pathogen *A. fumigatus* (Extended Data Fig. 3a,b).

Notably, *A. nidulans* conidia cultivated in an outdoor environment in different months, which had different weather conditions and day–night durations, were also highly variable (Fig. 2h), indicating that conidia in nature also have distinct transcription profiles. Taken together, these results not only demonstrate that conidia themselves can execute environment-specific transcriptional responses but also indicate that the experience of conidia during development and maturation can result in very different conidial transcriptome compositions. In addition, the observed transcriptional activity also indicated that fully developed conidia on conidiophores have not yet established dormancy.

Conidia on conidiophores are transcriptionally active long after the completion of development. We next used RNAP II binding as an assay to determine when conidia enter dormancy and become unresponsive to the environment. *A. nidulans* conidial development was completed within 3 d after inoculation[45] (Extended Data Fig. 5a). Unexpectedly, we found that the conidia on conidiophores were both transcriptionally active (Fig. 3a) and responsive

Fig. 1 | Filamentous fungal conidia have robust transcription activities by all three RNA polymerases. a, Representative genome browser screenshots showing RNAP II ChIP–seq signals in conidia and hyphae of *A. nidulans*, *A. fumigatus*, *T. marneffei* and input DNA distribution as a negative control over the indicated chromosome. **b**, A genome browser screenshot showing TBP, TFIIB and RNAP II ChIP–seq binding levels and locations at four representative genes for *A. nidulans* conidia. **c**, Heatmap plots showing ChIP–seq signals of elongation RNAP II, TBP and TFIIB for genes with detectable RNAP II level at their gene body. Gene order was ranked from high to low RNAP II levels. As a control, the same number (n = 1,030) of randomly selected genes with no RNAP II ChIP–seq signal (that is, non-transcribed) were plotted. **d**, Scatter plots showing the Pearson correlation analysis of RNAP II and TFIIB or TBP ChIP–seq signals at coding and promoter regions, respectively, for conidia. **e**, Scatter plots showing Pearson correlation analysis of RNAP II and TFIIB or TBP ChIP–seq signals at coding and promoter regions, respectively, for hyphae. **f**, A line plot showing the histone H3 level around the transcription start site of the top 2,000 genes ranked by high to low RNAP II levels and of 1,030 randomly selected control genes with no RNAP II ChIP–seq signal (same as the ones used in **d**). **g**, Heatmap plots showing the ChIP–seq signals of H3Ac, H3K4me3 and H3K36me3 histone modifications at RNAP II-occupied genes and at non-transcribed genes (same as the ones used in **d**) as a control. The histone modification ChIP–seq signals were normalized to histone H3 levels. **h**, Line plots showing the RNAP II ChIP–seq signal and RNA-seq signal for the top 2,000 genes ranked by high to low RNAP II levels. **i**, A genome browser screenshot showing input DNA read distribution and normalized ChIP–seq signals of RNAP I subunits (Rpa43^{HA} and Rpc40^{HA}), TBP^{MYC} and TFIIB^{MYC} at rDNA loci. **j**, Heatmap plots showing the ChIP–seq signals of RNAP III initiation factors (TBP^{MYC}, TFIIIB^{HA} and TFIIIC^{HA}) and RNAP III core subunits (Rpo31^{HA}, Rpc40^{HA} and Rpc11^{MYC}) at tRNAs and 5S rDNAs. TSS, transcription start site; TES, transcription end site. In **a**,**b** and **i**, numbers in parentheses represent the *y*-axis scale range of normalised ChIP–seq read counts set on the IGB genome browser for the screenshot.

to the environment (Fig. 3b), even two weeks after completion of conidial development. The observed transcriptional activity was not due to newly synthesized conidia since both conidia number (Fig. 3c) and viability (Fig. 3d) were unchanged after 3 d of conidiation. Importantly, conidia of different ages had overlapping but non-identical sets of actively transcribed genes (Fig. 3e,f), which

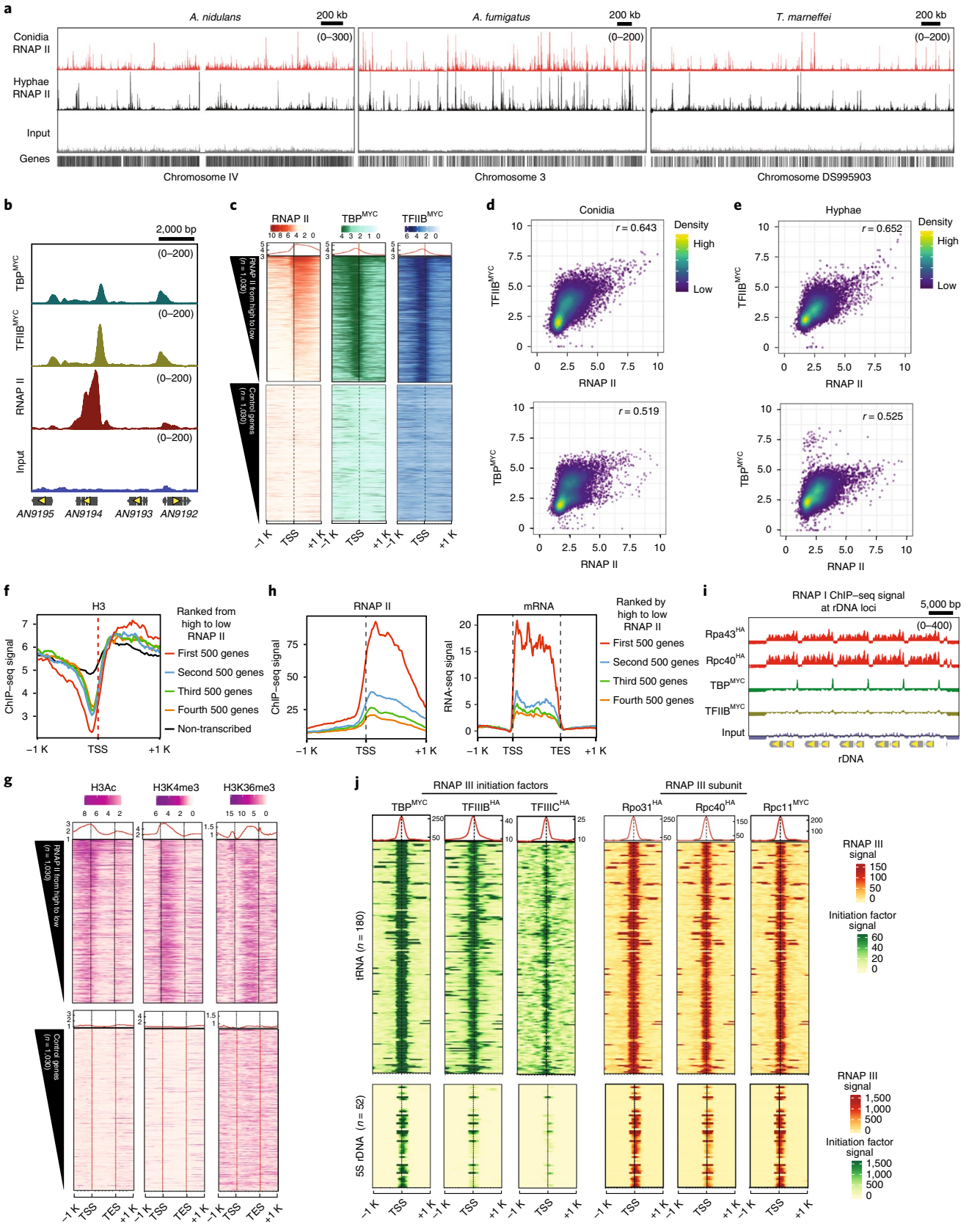

is consistent with the finding that *A. niger* conidia transcriptome changes with conidia age[21].

To further confirm that conidia on conidiophores are not dormant, we performed another assay to monitor cellular activities. Because conidia are believed to have very low[29,36] or no[2,34,35] metabolic activity, they are expected to have minimal ATP synthesis. We reasoned that intracellular ATP levels would decline over time if conidia were active until dormancy was established. Consistent with the transcription assay, the ATP levels in conidia continuously decreased throughout the experiment (Fig. 3g). The same results were obtained in the pathogenic species *A. fumigatus* for transcription, conidia numbers, conidia viability and ATP levels (Extended Data Fig. 4a–f). Combined, our results suggested that *A. nidulans* and *A. fumigatus* conidia are not dormant while on their conidiophores, even long after development is complete.

Dormancy is established after conidia detach from conidiophores. Conidia can remain dormant for years when collected from conidiophores and kept dehydrated at room temperature[1,2], whereas the viability of conidia that come into contact with water[36] or are kept on culture plates (that is, remain on conidiophores)[20] markedly decreases. We proposed that a connection exists between ATP levels, the establishment of dormancy and conidia separation from conidiophores. Conidia remaining on conidiophores are active and responsive to the environment and intracellular ATP levels are depleted to a level that is not sufficient to sustain cellular function or support germination, whereas separation from conidiophores might trigger the establishment of dormancy (for example, ceasing ATP-consuming cellular activities). Indeed, when conidia remained on conidiophores, the amount of intracellular ATP continued to decline over time, eventually reaching the background level after approximately 40–50 d (Extended Data Fig. 5b). ATP depletion was accompanied by a loss of germination ability (Extended Data Fig. 5c) and chromatin deterioration (Extended Data Fig. 5d), demonstrating a link between intracellular ATP levels and conidial viability. Most importantly, for both *A. nidulans* and *A. fumigatus*, intracellular ATP levels did not decline when conidia were separated from their conidiophores (Fig. 3h).

As an independent confirmation, we monitored the turnover of the developmental regulator protein WetA across conidia of different ages in *A. nidulans* (Fig. 3i). WetA turnover could be suppressed by separating conidia from conidiophores (Fig. 3j), indicating that separation can indeed arrest cellular activities. Moreover, separated conidia could no longer elicit a heat-shock transcriptional response (Fig. 3k) and the conidial transcriptome was unchanged after separation (Extended Data Fig. 5e). Cellular arrest may be due to a loss of an unknown signalling mechanism between conidia and the rest of the developmental structures after separation or merely an indirect consequence of dehydration that inhibits cellular activities. Notably, separated conidia suspended in water could still respond to heat shock (Fig. 3k), suggesting that conidia dormancy is likely triggered by dehydration.

Conidial transcripts serve functions during conidia development and maturation and can influence conidia composition. We next asked why conidia on conidiophores would invest their limited energy (for example, ATP levels) in sustaining transcriptional activities and what purpose this would serve. Active transcription in fungal conidia is probably a general phenomenon since transcripts have been reported to be present in the conidia of various fungi[1,21,27–34]. Previous studies[1,28,29,34,37,46] suggested a model where a pool of transcripts is prepackaged in conidia, with some transcripts functioning during conidial development and maturation and others for priming of translation after germination. In support of the developmental functions, many conidial developmental and maturation genes, which are controlled by the conidial developmental regulators WetA and AtfA[38,47] (Extended Data Fig. 6a), have high levels of elongating RNAP II and transcripts (Extended Data Fig. 6b,c).

The conidia of *Aspergillus* exposed to different conidiation conditions and of different ages are phenotypically heterogeneous[4,6,13,17,21,48–50]. We hypothesized that a condition-specific transcriptional response elicited in conidia can modulate phenotypic variations. Indeed, genes involved in the biosynthesis of conidial contents and transporter-encoding genes had highly variable levels of transcription among conidia exposed to different conidiation conditions (Fig. 2f,g and Extended Data Figs. 7a–d). Consequently, these differential transcriptions (for example, zinc and sugar transporter-encoding genes in zinc-starved conidia and NaCl conidia, respectively) led to different levels of conidial transcripts and proteins (Fig. 4a,b and Extended Data Fig. 7e). Therefore, conidia obtained from different environmental conditions are decorated with unique sets and levels of membrane transporters and thereby possess distinct nutrient and ion uptake capabilities.

Transcriptional variations for genes encoding surface and intracellular proteins and cell membrane transporters were also observed in *A. fumigatus* (Extended Data Fig. 7f). Interestingly, genes required for the biosynthesis of gliotoxin, a mycotoxin with immunosuppressive properties[51] that contributes to *A. fumigatus* virulence[52], were specifically transcribed in zinc-starved conidia (Fig. 4c). Chemical analysis showed that gliotoxin was indeed produced and stored inside zinc-starved conidia but not in control conidia (Fig. 4d,e), providing a direct link between conidial transcriptional events and cellular contents. Combined, the results not only demonstrate the functional significance of conidial transcriptional activities during conidial development and maturation but also provide a mechanistic basis for how genetically identical conidia achieve phenotypic variation.

Conidial transcripts expedite protein expression and molecular responses during germination. Notably, two groups of transcripts were identified based on the presence or absence of the respective proteins in conidia. For example, proteins with housekeeping (for example, histone H3, Hsf1 and factors of the transcription machinery) and conidial maturation (for example, WetA and AtfA) functions were readily detected in conidia (Extended Data

Fig. 2 | *A. nidulans* conidia on the conidiophores have distinct transcriptional profiles under different growth conditions. a, Representative genome browser screenshots of RNAP II ChIP–seq signals at representative genes for *A. nidulans* conidia subjected to cold (4 °C) and heat (42 °C) shocks. Representative genes are selected as differentially expressed between conidia under cold or heat shock. **b**, Heatmap plot showing differential gene expression (presented as *z*-scores) between conidia exposed to temperature shocks (4 and 42 °C) or not (37 °C). **c**, Representative genome browser screenshots of RNAP II ChIP–seq signals at selected genes for *A. nidulans* conidia formed under ANM medium (control conidia) with 0.5 M of KCl (KCl conidia), 0.5 M of NaCl (NaCl conidia) or ANM medium without zinc (zinc-starved conidia). Numbers in parentheses represent the *y*-axis scale range of normalised ChIP–seq read counts set on the IGB genome browser for the screenshot. **d**, Heatmap plot showing differential gene expression (presented as *z*-scores) between conidia formed under different growth conditions (control, NaCl, KCl or zinc-starved). **e**–**g**, Box plots showing expression of heat shock and control genes in conidia subjected to cold and heat shocks (**e**), zinc limitation response and control genes in conidia formed under zinc-deprived condition (**f**) and mitochondria electron transport, glycerol transport and metabolism and control genes in conidia grown in the presence of NaCl (**g**). **h**, MA plots showing pair-wise comparisons of RNAP II ChIP–seq signals of selected genes, which had differential RNAP II binding signals in at least one of the three comparisons, between *A. nidulans* conidia exposed to an outdoor environment in August, September or November 2020.

Fig. 8a). In contrast, a group of genes with functions in stress and environmental responses (for example, *areB*, *sreA*, *creA*, *amdX*, *pacC*, *rlmA* and *sfgA*) had levels of elongating RNAP II and mRNA similar to those of the housekeeping genes (Extended Data Fig. 8b and Supplementary Table 5); however, the corresponding proteins could not be detected in the conidia (Extended Data Fig. 8a).

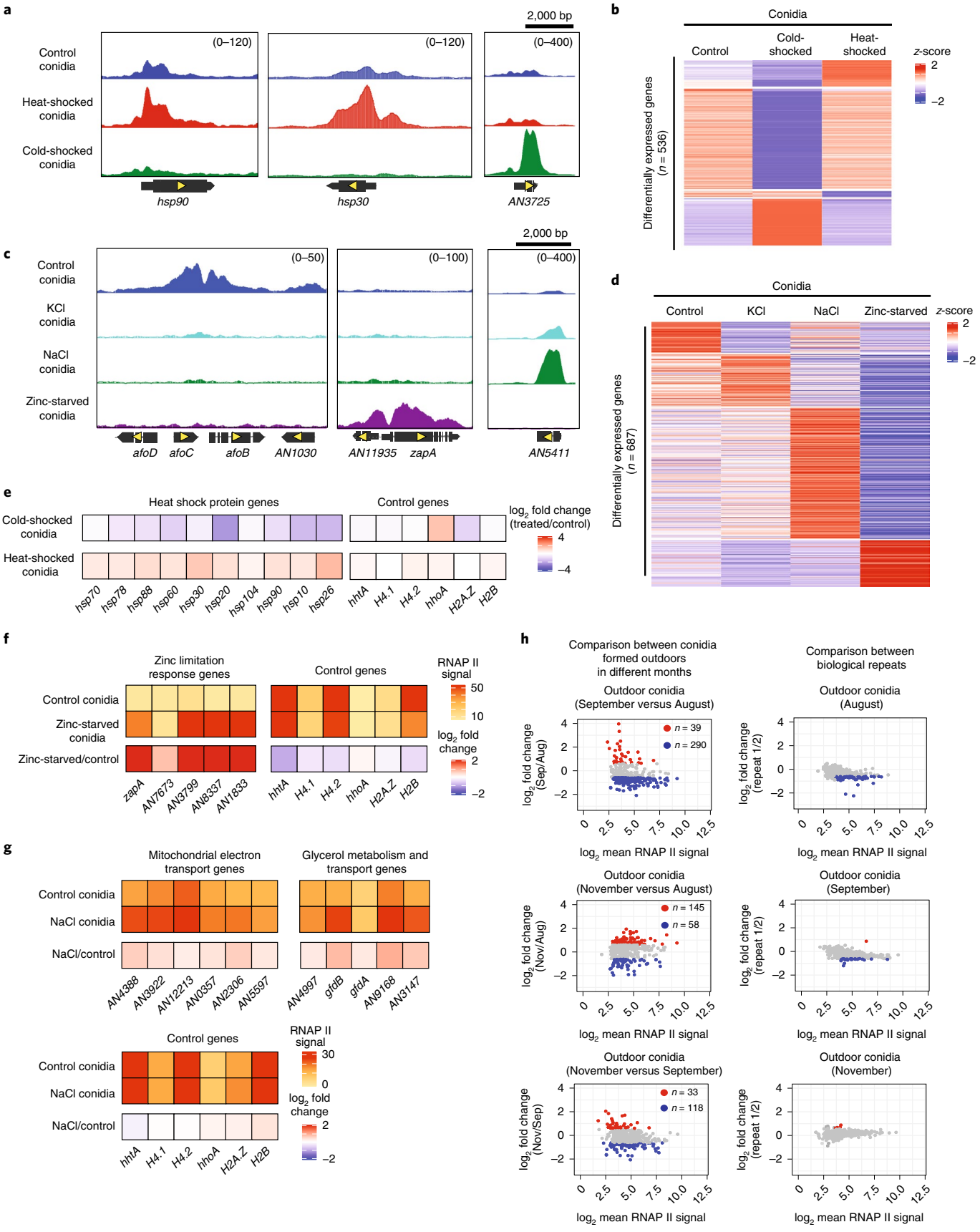

The disparity between transcriptional and protein levels observed in this study and by others[1,34,46] suggests that certain conidial transcription events are for translation later on in germination.

This is indeed the case for the *hsp70* chaperone gene and the *zapA* transcriptional regulator gene. In both cases, increased transcription of *hsp70* (Fig. 2e) and *zapA* (Figs. 2f and 4a) in heat-shocked

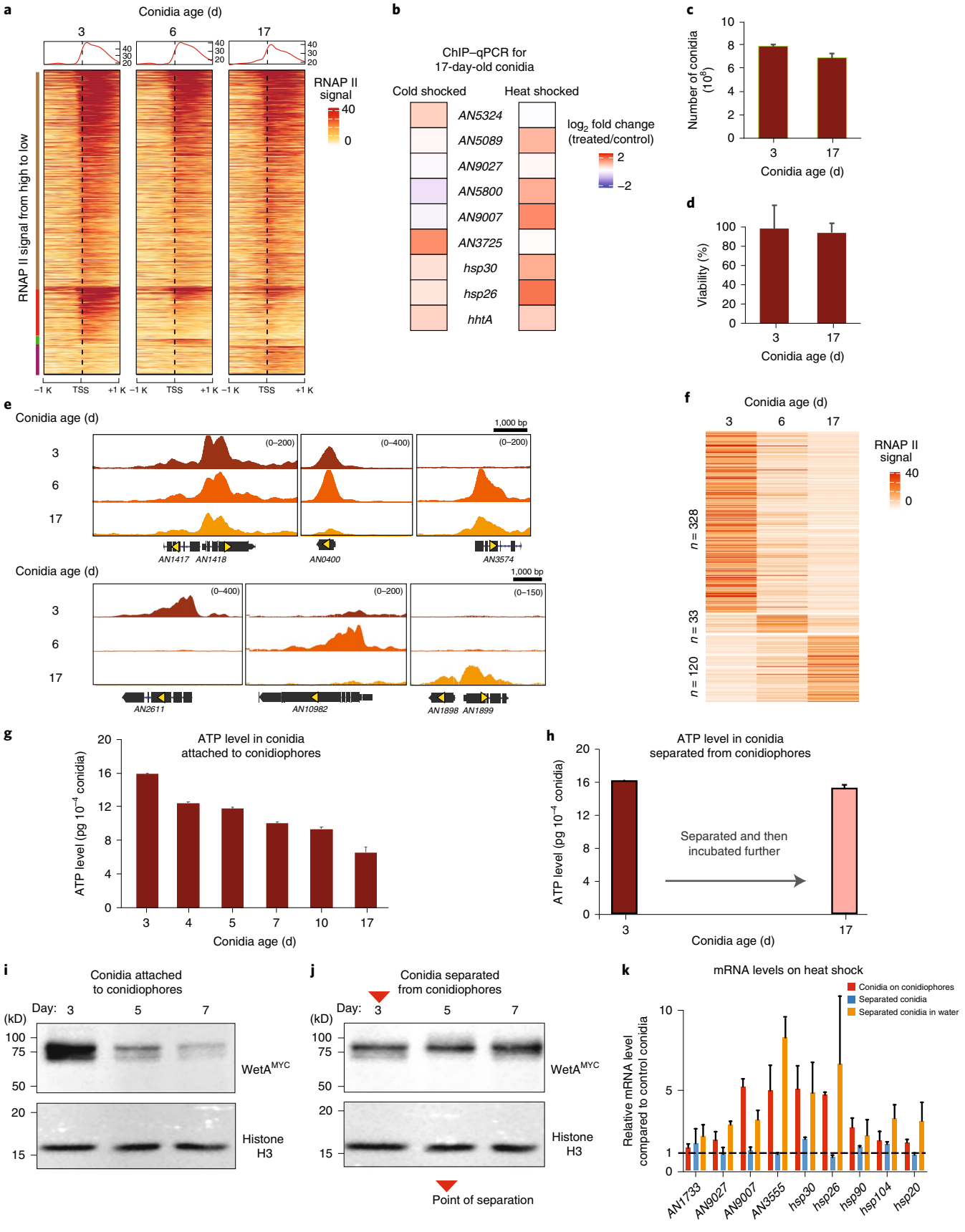

Fig. 3 | *A. nidulans* conidia remain active until release from the developmental structure (conidiophore). a, Heatmap plots showing RNAP II ChIP–seq signals on transcribed genes for conidia of different developmental ages (for example 3-, 6- and 17-day-old conidia). **b**, Expression changes of selected genes as measured by ChIP–qPCR against RNAP II for 17-day-old conidia subjected to cold (4 °C) or heat (42 °C) shock. **c**,**d**, Bar plots showing the number of conidia (**c**) and viability of 3- and 17-day-old conidia cultures (**d**). Data are presented as the mean + s.d. The error bars represent the s.d. of three independent experiments. **e**, Genome browser screenshots showing RNAP II ChIP–seq signals on representative genes for 3-, 6- and 17-day-old conidia to illustrate their differential transcription events. Numbers in parentheses represent the *y*-axis scale range of normalised ChIP–seq read counts set on the IGB genome browser for the screenshot. **f**, Heatmap plot showing the RNAP II ChIP–seq signal of differentially expressed genes ($n = 481$) among conidia of different developmental ages. **g**,**h**, Bar plots showing ATP level in conidia of different developmental ages (for example 3, 4, 5, 7, 10 and 17-day-old) (**g**) or in 3-day-old conidia separated from the conidiophore (**h**) and further incubated on a filter paper at the same temperature as the conidia in **g** for another two weeks. Data are presented as the mean + s.d. The error bars represent the s.d. of three independent experiments. **i**,**j**, Western blots showing WetA and histone H3 levels in conidia over time (for example, 3, 5 and 7 d) with (**j**) and without (**i**) separating conidia from conidiophores. The red triangle indicates the time of separation (day 3). The western blot experiments were repeated independently three times with similar results. **k**, Bar plot showing the transcript level of heat-shock response genes by RT–PCR after heat treatment (4 h) of conidia attached to (red bar) and separated (blue bar) from the conidiophores or separated but kept in water (orange bar). Data are presented as the mean + s.d. The error bars represent the s.d. of three independent experiments ($n = 3$). The two-tailed *P* value was calculated using an unpaired *t*-test with a 95% confidence interval.

and zinc-starved conidia, respectively, markedly promoted their protein expression and levels during germination without detectably altering their protein levels in conidia (Fig. 4f,g and Extended Data Fig. 9a,b). More importantly, during germination under zinc-limited conditions, zinc-starved conidia could produce faster molecular responses (induction of *zapA* and its downstream target genes) than control conidia (Fig. 4h,i). Therefore, conidial transcripts, especially those encoding protein products with regulatory functions, can influence molecular responses after germination. It is noteworthy that the transcription levels of many other transcription factor-encoding genes were also highly variable between conidia exposed to the four different environmental conditions analysed in both *A. nidulans* ($n = 61$) (Fig. 4j) and *A. fumigatus* ($n = 48$) (Extended Data Fig. 9c). These transcriptional differences may result in conidia developed under different environments possessing extremely heterogeneous molecular responses after germination. Overall, our results suggest that conidia actively synthesize specific mRNAs according to their environmental experience while remaining on the developmental structure so as to facilitate future germination responses.

Differences in conidial transcriptional responses during conidiation are responsible for phenotypic variation after germination. It is conceivable that heterogeneous compositions of transcriptomes, proteomes and cellular contents in conidia could have growth and physiological consequences after germination. Indeed, conidia formed under different conidiation conditions or of different ages had dissimilar germination behaviours in both *A. nidulans* (Extended Data Fig. 9d–g) and *A. fumigatus* (Fig. 5a,b). Conidiation conditions also affected the virulence of genetically identical *A. fumigatus* conidia in a *Galleria* larvae infection model (Fig. 5c).

We hypothesized that differences in conidia transcriptional responses during development and maturation are an important determinant of phenotypic variation. If this were true, we would be able to predict affected physiological processes from conidial transcription profiles. Indeed, several striking examples were identified for both *A. nidulans* and *A. fumigatus*. In one example, *A. nidulans* conidia that formed in high-osmolarity medium (NaCl conidia) had higher expression of many oxidative stress response genes (Extended Data Fig. 10a) and displayed increased tolerance to H_2O_2 compared with control conidia that formed under normal conditions (Fig. 5d). These NaCl conidia also had higher transcription levels of ergosterol biosynthesis genes (Extended Data Fig. 10b) and improved tolerance to high concentrations of azole-related antifungal drugs, which inhibit ergosterol biosynthesis[53] (Fig. 5e and Extended Data Fig. 10c). In contrast, no effect was found for the other antifungal drugs caspofungin and flucytosine that act via blocking glucan and DNA/RNA biosynthesis, respectively (Extended Data Fig. 10d).

In *A. fumigatus*, all the gliotoxin biosynthesis genes (Fig. 4c) and the genes required for protection against exogenous gliotoxin (Extended Data Fig. 10e) were specifically transcribed in zinc-starved conidia. Consequently, their growth was better protected against exogenously added gliotoxin when compared with control conidia formed under a standard, zinc-replete medium (Fig. 5f). Importantly, the hyphae grown from zinc-starved conidia produced and secreted gliotoxin much earlier and at a fivefold higher level than hyphae grown from control conidia (Fig. 5g and Supplementary Fig. 1). Notably, genes from other secondary metabolite biosynthetic clusters[54] were also transcribed at a higher level in zinc-starved conidia than in control conidia (Extended Data Fig. 10f) suggesting that conidia formed under different conditions may have dissimilar secondary metabolite production and

Fig. 4 | *A. nidulans* and *A. fumigatus* conidial transcription activity affects gliotoxin content in conidia and accelerates protein expression and molecular response on germination. a, Histogram showing the transcript levels of *zapA* and three *zapA* downstream target genes by RT–PCR in zinc-starved conidia compared with the control conidia of *A. nidulans*. $^*P < 0.05$. **b**, Western blot analysis showing the protein level of zinc transporters (AN3799, AN8337 and AN1833) in control and zinc-starved conidia of *A. nidulans*. Histone H3 was used as a loading control. **c**, Bar plot showing the transcription level (by RNAP II ChIP–seq) of gliotoxin biosynthesis cluster genes in *A. fumigatus* conidia formed under ANM medium in the presence (control conidia) or absence of zinc (zinc-starved conidia). **d**, Bar graph showing the gliotoxin level in *A. fumigatus* control and zinc-starved conidia. Data in **a** and **d** are presented as the mean + s.d. The error bars represent the s.d. of three independent experiments. The two-tailed *P* value was calculated using an unpaired *t*-test with a 95% confidence interval. $^{***}P < 0.001$. **e**, UPLC–MS signals for gliotoxin standard (0.67 μg ml^{-1}) or intracellular gliotoxin from WT *A. fumigatus* conidia conidiated in the presence (control conidia) or absence of zinc (zinc-starved conidia) as shown in **d**. **f**,**g**, Western blot showing the time-course analysis of Hsp70 protein in heat-shocked and cold-shocked conidia of *A. nidulans* on germination at 42 °C (**f**) and of ZapA protein in zinc-starved and control conidia before and during germination in the absence of zinc (**g**). Histone H3 was used as a loading control. The western blot experiments in **b**,**f**,**g** were repeated independently three times with similar results. **h**,**i**, Line plots showing the time-course RT–qPCR analysis of *zapA* (**h**) and three ZapA downstream target genes (**i**) in zinc-starved and control conidia of *A. nidulans* on germination under zinc-deficient conditions. The same trend was observed in the biological repeats. The raw data are presented in Source Data Fig. 4. **j**, Transcription levels for 61 transcription factor-encoding genes, which had detectable RNAP II ChIP–seq signals, in the zinc-starved, NaCl, KCl and control conidia of *A. nidulans*.

capacities after germination. These findings indicate that conidial transcripts can mould fungal capabilities and have effects even at later growth stages.

Artificial manipulation of the transcript levels of a transcription factor-encoding gene in conidia greatly enhances the capacity for secondary metabolite production. To directly demonstrate that

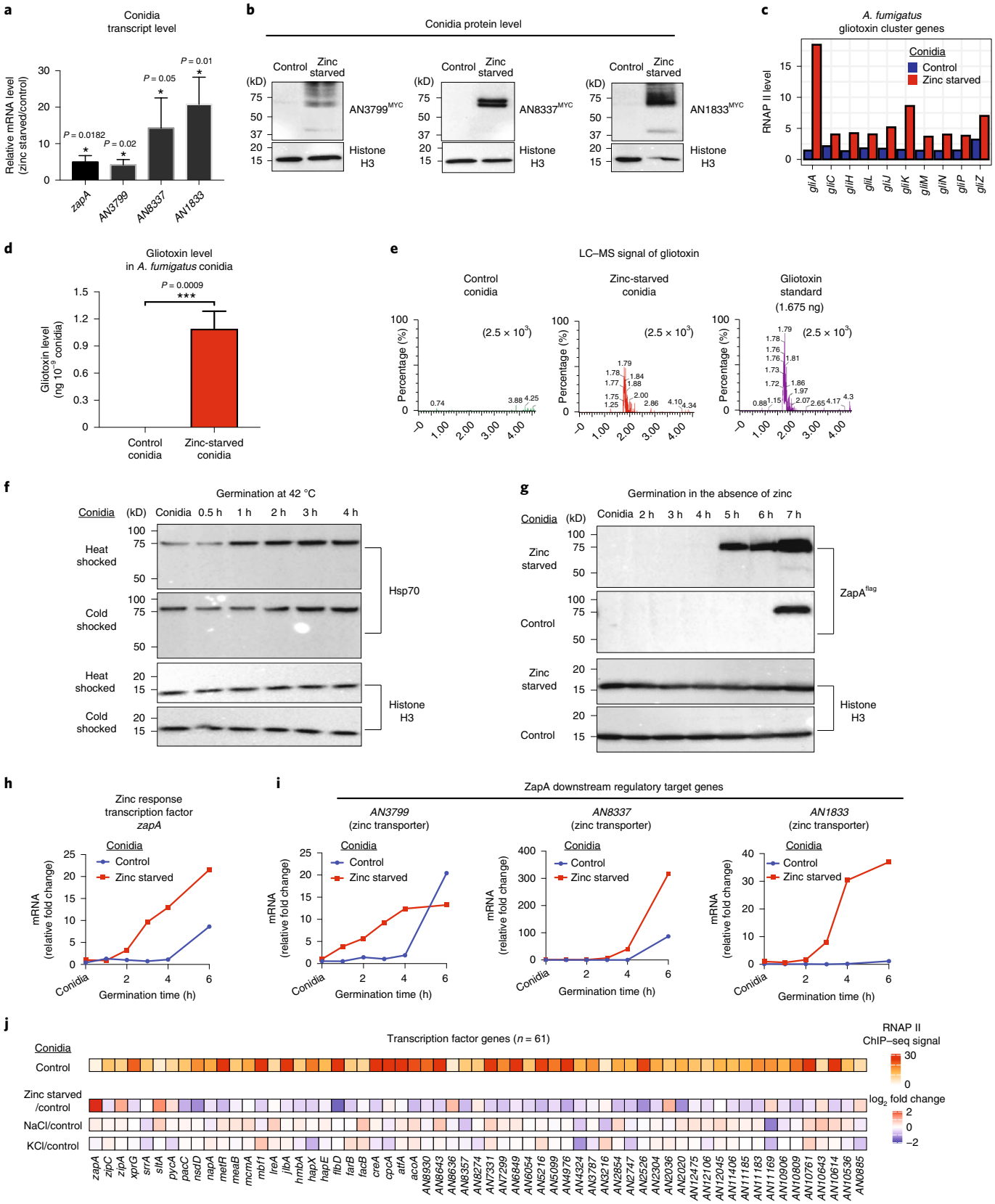

differences in conidial transcripts could drive phenotypic variations, we set up an artificial experimental system to conditionally upregulate a transcriptional regulator-encoding gene in conidia for a postgermination physiological process and then determined whether the outcome of the process could be changed. The system was established using sterigmatocystin production as a reporter because sterigmatocystin biosynthesis occurs several days after germination. Therefore, the artificial system could determine whether the conidia transcription effect also influenced physiologies long after germination. A mechanistic strain that can conditionally and strongly overexpress *aflR* (encoding the primary transcription factor of sterigmatocystin biosynthesis genes[55]) by the *xylP* promoter of *Penicillium chrysogenum*[56] was generated. Unexpectedly, the strong induction of *aflR* led to a complete lack of conidiation (Extended Data Fig. 10g) and the strain could not be used. Therefore, we created an *rsmA* overexpression strain, whose conidiation is normal, to upregulate the conidial *aflR* level[57]. Remarkably, when conidia with or without *aflR* upregulation (Fig. 5h) (referred to as induced and non-induced conidia, respectively) were assayed for sterigmatocystin production during vegetative growth 4 d after germination, there was a striking difference in sterigmatocystin levels in the culture media, with induced conidia producing approximately tenfold more sterigmatocystin than non-induced conidia (Fig. 5i,j). Although the *aflR* transcript levels were not significantly different at this stage (day 4), the expression of an AflR target gene (*stcA*) was higher in hyphae grown from induced conidia than in those grown from non-induced conidia (Fig. 5k), indicating stronger AflR activation presumably as a result of a greater abundance of the AflR protein. Therefore, this mechanistic experiment demonstrated an example of the differential expression of a transcription factor-encoding gene in conidia leading to a dramatic change in the outcome of a physiological process, even several days after germination, emphasizing the hitherto unknown importance of conidial transcription activity before dormancy.

Discussion

In this study, we revealed that *Aspergillus* conidia are highly proactive in their own development, eliciting specific transcriptional responses according to environmental conditions and thereby preparing for their future physiology and growth after germination. The observation that robust transcriptional activities occur in the conidia of three filamentous fungal species is surprising given the common view that conidia are dormant and that transcripts are synthesized in the conidiophore and packaged into individual conidia during development. Our results demonstrate that the transcriptional activity of conidia before dormancy (that is, the period between completion of conidia formation on the phialides and release into the environment) contributes to conidia maturation and has far-reaching effects on subsequent fitness and capabilities once they exit dormancy. This phenomenon potentially offers physiological advantages to conidia and provides a mechanism through which clonal conidia can achieve phenotypic variation. It is noteworthy that the mechanism and, therefore, phenotypic variation may also be influenced by the experience and heterogeneity of parental hyphae and other developmental cells as well as by epigenetic regulation[23].

How does the conidial transcriptome influence subsequent physiologies and modulate phenotypic variation? We and others[1,34,46] have observed disparities between conidial transcript and protein levels. This, together with our findings, suggests a model whereby specific transcripts (for example, transcripts coding for genes with conidia development, maturation and housekeeping functions) are translated in conidia, while others are not, or at most at very low levels (Fig. 6, circled item 1). Differences in the levels and composition of the former group of transcripts would alter their protein levels and functions in conidia (Fig. 6, circled item 2), thereby affecting conidia maturation and biosynthetic processes. Hence, conidial contents, such as surface and intracellular proteomes[4,6,48], membrane transporters (Fig. 4b and Extended Data Fig. 7e), trehalose[13,14,17,21], melanin[13], ergosterol and secondary metabolites (Fig. 4d and past[13,49] studies), would vary according to the conidia transcriptional response during maturation. Similarly, the differential transcription of regulatory genes (for example, transcription factor-encoding genes) would give rise to conidia carrying distinct combinations of transcripts and/or proteins (Fig. 6, circled item 3). Given that proteins in this class usually act on a large number of downstream genes, variations in the levels and functions of the proteins would potentiate differences in the transcriptome (Fig. 6, circled item 4) until conidia become dormant after separation from conidiophores or on dehydration.

At the break of dormancy, conidia rely on their existing transcriptome and proteome to resume growth[58]. For example, conidia expressing different membrane transporters would have dissimilar ion and nutrient uptake capabilities (Fig. 6, circled item 5) and germination behaviours[5,8,16–19,21]. Additionally, existing conidial transcripts could expedite protein expression, which would otherwise require de novo transcription (Fig. 6, circled item 6). As demonstrated for the transcription factor ZapA (Fig. 4g,h), a faster induction of transcriptional regulators could, in turn, accelerate the induction of downstream target genes and their functions (Fig. 6, circled item 7). We propose that the compendium of transcriptional regulator-encoding transcripts and their protein products in a conidium can shape the overall regulatory network and, consequently, the proteome of the conidium at the earliest stage of germination (Fig. 6, circled item 8). This, in turn, has consequential effects on subsequent physiology, including stress and drug

Fig. 5 | *A. nidulans* and *A. fumigatus* conidial transcription activity before dormancy affects germination, stress and drug resistance and secondary metabolite production capacity after germination. a,**b**, Line plots showing the germination kinetics of *A. fumigatus* conidia of different developmental ages (for example, 3- and 17-day-old conidia) (**a**) and formed under control, NaCl or zinc-starved conditions (**b**). **c**, Kaplan–Meier survival plot showing the survival of *G. mellonella* larvae over time after infection with *A. fumigatus* conidia formed on control, NaCl and zinc-deprived conditions. **d**,**e**, Growth tests of an *A. nidulans* WT strain on solid ANM medium containing different concentrations of hydrogen peroxide (0, 0.05 and 0.1% H_2O_2) (**d**) or the antifungal drug fluconazole (0, 32 and 256 μg ml^{-1}) (**e**) using NaCl or control conidia. **f**, Growth tests of an *A. fumigatus* WT strain on solid ANM medium with gliotoxin (50 μg ml^{-1}; +) or without (−) using control or zinc-starved conidia. **g**, Line plot showing gliotoxin levels (concentration) in the culture media inoculated with *A. fumigatus* control or zinc-starved conidia over a 5-d period. **h**, Histograms showing the RT–qPCR results of *aflR* transcripts level in *A. nidulans xylP*(p)*rsmA* conidia under an inducing condition compared to genetically identical conidia formed under a non-inducing condition. **i**, Bar plot showing the concentration quantification of sterigmatocystin in 4-d culture media for *A. nidulans* conidia of the *xylP*(p)*rsmA* strain conidiated under inducing (pre-induced conidia, induction with 1% xylose) or non-inducing (non-induced conidia) conditions. **j**, UPLC–MS signals for sterigmatocystin standard (4 μg ml^{-1}) or sterigmatocystin level in 4-d culture media as described in **i**. **k**, Histograms showing the RT–qPCR results of *aflR* and *stcA* transcript levels in 4-d hyphae of the *xylP*(p)*rsmA* strain grown from pre-induced or non-induced conidia. **a**–**c**,**g**–**i**,**k**, Data are presented as the mean + s.d. The error bar represents the s.d. from three independent experiments. *P* values were calculated using an unpaired *t*-test and are shown as a two-tailed value using a 95% confidence interval, except for **b** where a one-way analysis of variance with multiple comparisons test was used. $^{*}P < 0.05$, $^{**}P < 0.005$, $^{***}P < 0.001$, $^{****}P < 0.0001$. NS represents $P > 0.05$.

resistance and the production of secondary metabolites (Fig. 6, circled item 9). Therefore, the transcriptional activity before dormancy not only lays down a blueprint for cellular physiology at the early stages of germination but also affects subsequent conidial fate.

Recent single-cell studies have revealed that individual *A. fumigatus* conidia developed under identical growth conditions are highly heterogeneous[6,16]. Our work suggests that conidia heterogeneity is likely an intrinsic outcome of the conidium developmental and maturation process. Conidia are formed in chains, one after the other, and are, therefore, of different developmental ages at different parts of the chains. In light of our results that transcriptional profiles and intracellular ATP levels change with the age of conidia, it is conceivable that conidia originating from the same conidiophore are essentially heterogeneous with respect to these contents. This spatio-temporal effect potentially explains the germination heterogeneity observed among genetically identical *A. fumigatus* conidia

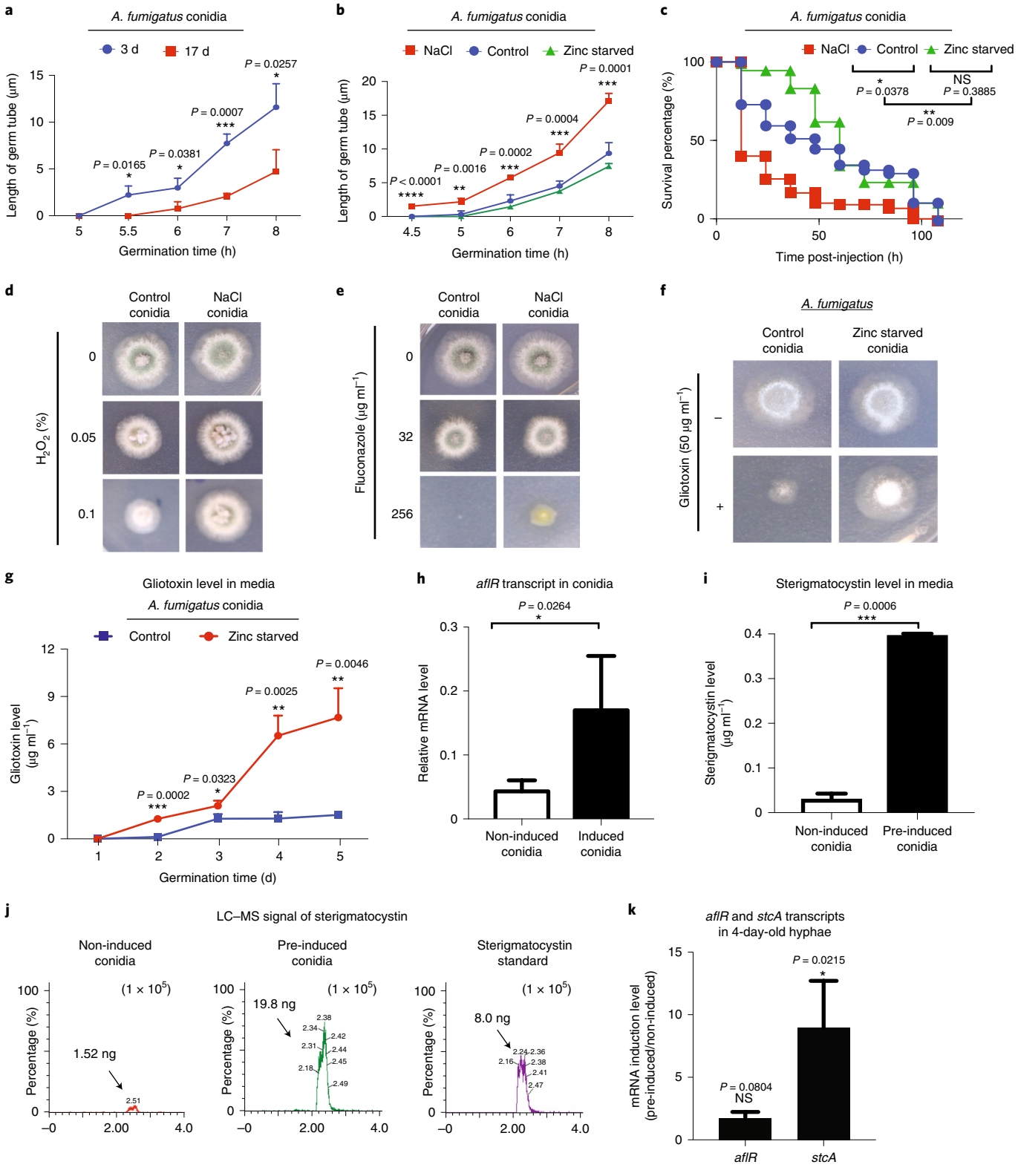

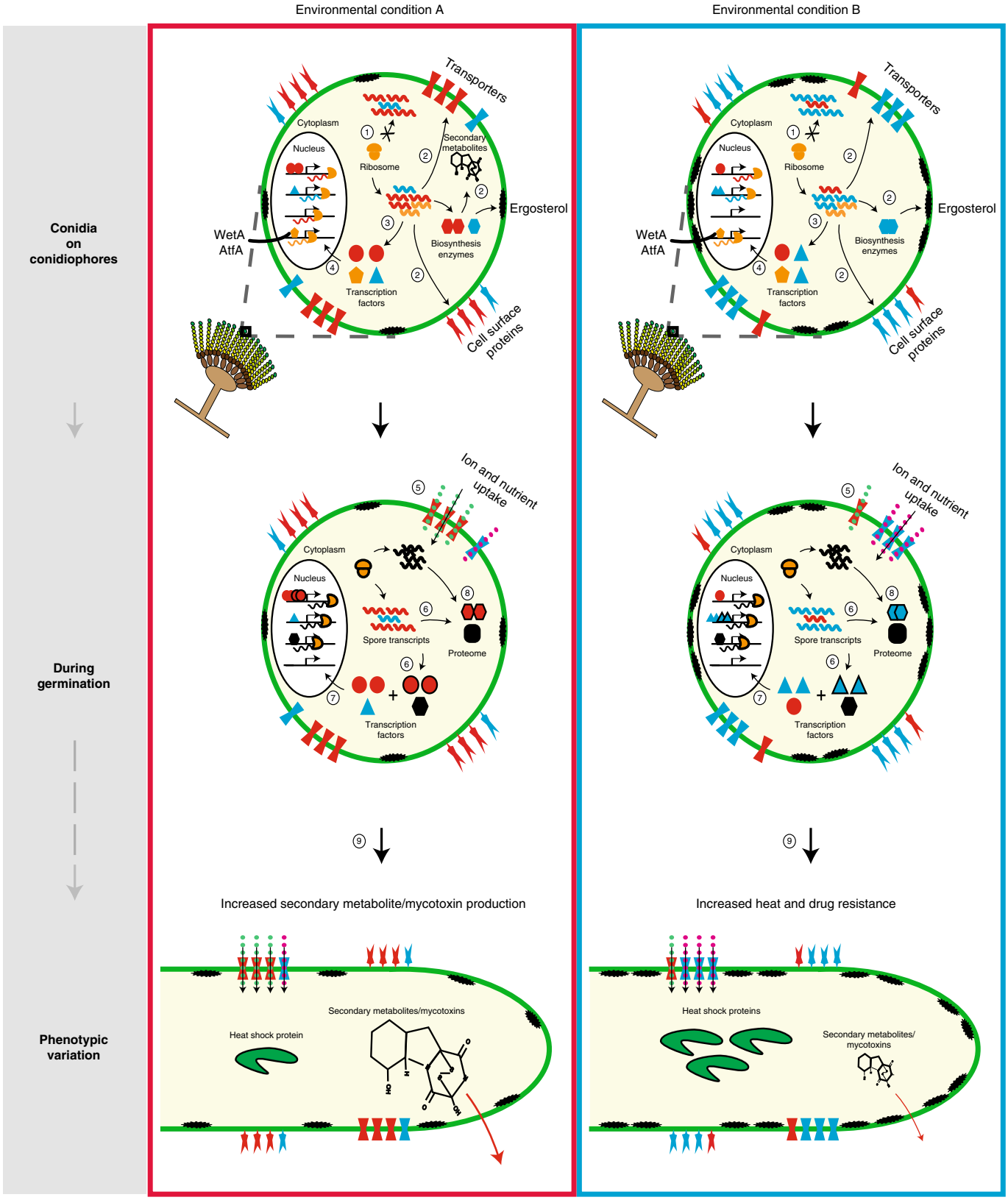

formed under the same conidiation conditions[16]. Given that transcriptional activity continues until conidia are separated from their conidiophores, we suggest that conidia maturation is a continuous and flexible, rather than a programmed, process. The timing of when conidia enter dormancy, which is triggered by dehydration, is critical for their fitness and viability since conidia may deteriorate when their intracellular ATP level is exhausted.

In nature, conidia are formed and mature under different substrates and environments and are dispersed erratically at different developmental ages. Consequently, they would have different

Fig. 6 | Proposed mechanism for how conidial transcription activity before dormancy drives phenotypic variation in conidia and in hyphae after germination. Schematic diagram showing the effects of conidial transcription activity towards conidia maturation and subsequent physiology after germination. During conidia development and maturation, conidia are transcriptionally active and responsive to the environment while remaining on the conidiophore. As a result, conidia developed under different environmental conditions (environmental condition A or B) transcribe different sets and/or levels of genes (annotated as red and blue transcripts in the figure). There are two groups of conidial transcripts based on their protein levels in conidia: (1) one group is synthesized for translation in conidia, while another class are mainly made for translation on germination; (2) for the former group, differences in transcript levels and compositions lead to variations in proteome composition (for example, cell surface proteins and transporters and biosynthesis enzymes) and hence physiological functions (for example, production of secondary metabolites); (3) similarly, the compendium of transcription factors also varies between conidia formed under different environments; (4) this in turn causes variations in the expression of their respective downstream target genes, potentiating gene expression heterogeneity between the two conidia. Therefore, they possess dissimilar cell surface and intracellular proteome compositions and chemical contents; (5) with these marked differences, those conidia are not expected to have the same physiological functions during germination. For example, differences in cell surface transporters are likely to affect their ion and nutrient uptake efficiency and, consequently, germination behaviour; (6) at the same time, those conidial transcripts that are not or are lowly translated in conidia can now be translated to accelerate protein expression during germination; (7) faster expression of transcription regulators can quicken molecular responses, which in turn can influence the physiological response of germinating cells; (8) in cases when the set of transcription regulators and/or proteome composition differs between conidia, different molecular responses and physiological functions might be executed; (9) this leads to phenotypic variation (for example, mycotoxin production, stress and drug resistance) after germination.

transcriptional responses and maturation statuses, giving rise to dissimilar molecular, physical and physiological properties. We propose that conidial transcriptome heterogeneity is an important mechanism for surviving the diverse environmental conditions in the wild. Indeed, altering the asexual developmental gene expression programme is a natural strategy for evolving new conidial properties[22].

This work has profound implications for fungal research, infection and biology. From the research perspective, our findings suggest that the use of different conidiation conditions within and across laboratories could lead to inconsistent experimental results. Therefore, it is necessary to standardize growth conditions for conidia preparation. It is also important to always consider potential conidial effects when interpreting mutant phenotypes; this is especially true for mutants expected to have an altered conidial transcriptome due to transcriptional dysregulation or altered growth and developmental rates that, in turn, affect conidial maturation states. For fungal infection studies, this work also raises a conundrum as to how much of what we learn from laboratory-propagated conidia of fungal pathogens can be extrapolated to conidia formed under dynamic natural environments. Importantly, our results suggest that conidia formed under different substrates (for example, soil, compost, an animal carcass or an infected plant) and/or environmental conditions (for example, cold or hot) may possess inherently dissimilar physiologies and contents (for example, the immunosuppressive compound gliotoxin) with consequences for their pathogenicity. This is supported by a recent study showing a relationship between conidia heterogeneity and susceptibility to macrophage phagocytosis[6] and begs the daunting question as to which sporulation conditions in nature yield the most pathogenic conidia for the different plant and human fungal pathogens. Besides infection-related studies, the striking effect observed for the biosynthesis of the carcinogenic secondary metabolite sterigmatocystin in the mechanistic experiment also demands careful consideration of the effect(s) of conidial preparation in secondary metabolism research, which holds promise for drug discovery. This observation also suggests the potential of manipulating the conidial transcriptome for enhancing secondary metabolite (that is, drug) production efficiency in the pharmaceutical and biotechnological industries. Finally, from the biology point of view, our results also suggest a fascinating phenomenon related to how fungal conidia prepare for their future before entering into dormancy. This ability offers conidia a head start in germination under environmental conditions similar to what they originated from, without compromising their ability to germinate in a different environment. Although it may be difficult to generalize this phenomenon to all fungi given the diverse differences in their developmental programmes[59], we anticipate that evolution would have selected for such an advantageous phenomenon in many, if not all, spore-forming fungi; it will be interesting to see whether a similar mechanism exists in other organisms that establish dormancy.

Methods

Strains and culture conditions. The strains used are listed in Supplementary Table 6. Epitope-tagged strains were constructed as described previously[60]. A schematic diagram illustrating the preparation of conidia for the ChIP–seq experiments is presented in Supplementary Fig. 2. For all experiments except where otherwise indicated, conidiation was induced by spreading and growing conidia on solid media containing 2% agar at 37 °C for 3 d in the presence of light. For the conidia age experiments, conidia were grown on complete medium for the indicated number of days, while *Aspergillus* nitrogen-free minimal (ANM) medium[61] containing 1% glucose and 10 mM of ammonium tartrate was used for the experiments involving 0.5 M of NaCl, 0.5 M of KCl and zinc-free conidiation conditions. Heat and cold shock of conidia were performed by transferring plates of 3-day-old conidia grown on complete medium from 37 °C to 42 °C or 4 °C, respectively, for 4 h. For the outdoor conidiation experiment, inoculation was performed as described in Supplementary Fig. 2 and culture plates in duplicate (that is, biological repeats) were grown at 37 °C for 1.5 d before moving to an outdoor environment for another 1.5 d. This experiment was repeated 3 times in different months in 2020 (for example, 15–18 August, 2–5 September and 7–10 November). For the *rsmA* overexpression experiments, conidia were grown on ANM medium with or without 1% xylose and collected 2 d after spread inoculation. For the liquid culture experiments, conidia were inoculated in 100 ml of ANM medium containing 1% glucose and 10 mM of ammonium tartrate at 37 °C in an orbital shaking incubator at 220 r.p.m. for the indicated amount of time. The conidiation conditions analysed in this study are summarized in Supplementary Table 7.

Conidia collection. Conidia were collected by scraping in 5 ml of 0.01% Tween 80. The conidial suspension was vortexed, washed twice with sterile water to remove trace amounts of Tween 80 and passed through a 40-μm nylon mesh sterile filter (catalogue no. 22-363-547; Fisherbrand) twice to separate conidia from mycelia mass and debris before counting. Conidia were then pelleted using low-speed centrifugation (for example, 3,000 r.p.m.) at 4 °C for 3 min and used for the indicated experiments. For ATP measurements in conidia separated from conidiophores, pelleted conidia were transferred onto sterile filter paper and incubated at 25 °C alongside with corresponding non-separated conidia on plates for the indicated number of days.

Chromatin preparation. One per cent formaldehyde solution (diluted in 0.01% Tween 80) was added directly to conidia on a plate. Conidia were collected by scraping and the conidial suspension was transferred to a 50-ml sterile Falcon tube and incubated at room temperature with gentle shaking for 20 min. Subsequently, glycine was added at a final concentration of 0.5 M and the mixture was further incubated at room temperature for 10 min. Cross-linked conidia, which were tested inviable by the colony-forming unit assay (Supplementary Fig. 3a), were collected as described above. Conidial pellets were washed twice with ice-cold water, snap-frozen in liquid nitrogen and stored at −80 °C until use. Cross-linked conidia were freeze-dried for at least 3 h and lysed by 6 × 3 min beating using a Bullet Blender (Next Advance) with at least 3 min of cooling in between each

cycle. Chromatins were extracted as described for hyphae[62] and sonicated using the Qsonica Q800R at 100% amplitude with 10 s ON and 15 s OFF cycles for a total sonication time of 30 min. The lysis efficiency of cross-linked conidia of different developmental ages (that is, 3, 6 and 17 d after inoculation) were comparable as determined by real-time PCR analysis of the amount of extracted chromatin DNA (Supplementary Fig. 3b). Chromatin size (approximately 100–500 base pairs (bp)) and quality were checked on a 2% agarose gel. Chromatins were stored at −80 °C until use.

ChIP–seq library preparation. Immunoprecipitation was carried out as described by Wong and Struhl[63] using antibodies listed in Supplementary Table 8. The amount of antibody used for ChIP–seq is shown in the table. Immunoprecipitated materials were purified using the QIAGEN PCR Purification Kit (catalogue no. 28106) and a small fraction (approximately 2 µl) was diluted for quality checking by real-time PCR. The rest of the sample was subjected to library preparation as described previously by Wong et al.[64] except for the end-repair step using the NEBNext Ultra II End Repair/dA-Tailing Module (catalogue no. E7546L; New England Biolabs) accordingly to the manufacturer's protocol. For the input controls, 1 ng of chromatin DNA was used for library preparation. Libraries were checked and quantified using the DNA High Sensitivity Bioanalyzer assay (catalogue no. XF06BK50; Agilent Technologies), mixed in equal molar ratio and sequenced using the Illumina HiSeq 2500 platform at the Genomics and Single Cells Analysis Core facility at the University of Macau.

RNA extraction and preparation for RNA sequencing. Conidia (1×10^9) were suspended in ice-cold 0.01% Tween 80, filtered twice using a 40-µm sterile filter and pelleted by centrifugation for 3 min at 3,000 r.p.m. at 4 °C. The pellet was washed twice with ice-cold water followed by freezing in liquid nitrogen. Hyphae were collected using a miracloth, washed, press-dried and snap-frozen in liquid nitrogen. One millilitre of TRIzol (catalogue no. 135405; Ambion) was added to 30 mg of mycelial or conidial sample for RNA extraction through 6 cycles of beating with approximately 100-µl volume of silica beads using a Bullet Blender. RNA was extracted as described by Rio et al.[65]. RNA quality was checked using the RNA Nano Chip (catalogue no. WJ04BK20) on an Agilent Bioanalyzer 2100. All RNAs used had a minimum RNA integrity number of 7.0. Sequencing libraries were prepared using the Illumina ScriptSeq Complete Gold Kit (Yeast) (catalogue no. BGY1324) according to the manufacturer's protocol.

Real-time quantitative PCR with reverse transcription. One microgram of total RNA was subjected to reverse transcription into complementary DNA using the PrimeScript RT reagent Kit with gDNA Eraser (catalogue no. RR047A; Takara Bio) according to the manufacturer's protocol. The resultant cDNA samples were diluted 20-fold and 2 µl of diluted samples were subjected to real-time quantitative PCR with reverse transcription (RT–qPCR) analysis using Premix Ex Taq DNA polymerase (catalogue no. RR039W; Takara Bio) and the primers listed in Supplementary Table 9 on an ABI Fast 7500 (Applied Biosystems) Real-Time PCR machine. The $\Delta\Delta^{Cr}$ method was used for quantification with respect to the histone gene *hhtA* as an internal reference.

Bioinformatics analysis. The raw sequencing reads of the ChIP–seq experiments were quality-checked using FastQC (http://www.bioinformatics.babraham.ac.uk/projects/fastqc/) and aligned to the reference genomes (for example, *A. nidulans* FGSC A4 reference genome version s10-m04-r03, *A. fumigatus* Af293 reference genome version s03-m05-r06 and *T. marneffei* ATCC18224 reference genome release 33) using Bowtie2 v.2.2.9 (ref. [66]). The RNAP I, II and III ChIP–seq signal (expressed as fragments per kilobase of transcript per million mapped reads (FPKM)) was calculated by first summing the number of sequencing reads on the respective genomic features (for example, 5.8S, 18S and 28S ribosomal DNA for RNAP I, coding regions for RNAP II and tRNAs and 5S rRNAs for RNAP III) and then normalizing to the length of features and total number of mapped reads. Since the *A. nidulans* FGSC A4 reference genome does not contain annotations for rDNAs, an unpublished improved version of the *A. nidulans* genome annotation (Aspnd5rm_Manual_Curation_2018_08_07.gff3; A. Tsang, unpublished) was used for the RNAP I bindings at 5.8S, 18S and 28S rDNAs (Extended Data Fig. 1i). For the RNAP III binding levels at the 5S rDNA locus (Extended Data Fig. 1h), which is still absent in the improved *A. nidulans* annotation, reads mapping to the 5S rDNA locus of *A. niger* CBS 51388 genome annotation (version s01-m07-r09) was counted and presented. ChIP–seq signals for histone and histone modifications were measured by first counting the number of reads at each base pair across specified regions; the numbers were normalized to the total number of mapped reads. For ChIP–seq against the TBP, TFIIB and RNAP III initiation factors and transcription factors, MACS 2 v.2.1.1(ref. [67]) was used for peak calling to identify their genomic binding locations. Peaks with $P < 0.05$ were assigned to their closest annotated genes using an in-house script (https://github.com/zqmiao-mzq/closest_gene_calling/blob/master/closest_gene_calling_v10.pl) and regarded as the targets. For RNA sequencing (RNA-seq), raw reads were aligned to the *A. nidulans* FGSC A4 reference genome (version s10-m04-r03) using hisat2 v.2.1.0 (ref. [68]). The expression level (for example, FPKM) for each annotated gene was calculated using Stringtie v.1.3.3b (ref. [68]). Gene ontology (GO) enrichment analysis[69] for *A. nidulans* and *A. fumigatus* was performed on the FungiDB (https://fungidb.org)[70], whereas the *A. nidulans* GO database was used for the analysis of *T. marneffei* ATCC18224 (FungiDB release 41) annotated genes due to limited GO information being available for *T. marneffei*. For each *T. marneffei* gene, the most probable *A. nidulans* orthologue was identified by a standalone BLASTx program v.2.8.1+. Only top hits with a query coverage and percentage identity >60% and *e*-value < 0.05 were considered as putative orthologues. GO analysis outputs were plotted using an in-house script (https://github.com/sethiyap/FungalSporeAnalysis) in RStudio v.1.0.153 or the online Bioinformatics analysis platform FungiExpressZ (https://cparsania.shinyapps.io/FungiExpresZ/).

Conidial germination assay. A total of 2.4×10^5 conidia were inoculated with 150 µl of ANM medium containing 1% glucose and 10 mM of ammonium tartrate in 1 well of a flat bottom 96-well plate and were grown at 37 °C. Two microscopic images were taken through a 40× objective for each well every 30 min for 16 h using the Cytation3 Cell Imaging Multi-Mode Reader (BioTek). The emergence of the germination tubes was monitored over time and their length was measured using ImageJ v.1.5.0i (ref. [71]). Approximately 150–250 conidia were counted for each experiment and three independent experiments were carried out for each conidia preparation.

Conidial viability assay. Three or 17-day-old conidia were resuspended in 0.01% Tween 80 and vortexed for at least 15 s. Approximately 100 conidia were evenly spread onto 3 plates of solid complete medium[61] containing 0.01% Triton-X100 [72] and grown at 37 °C for 2 d. Conidial viability was calculated by dividing the number of arising colonies by the number of inoculated conidia and expressed as a percentage. Approximately 300 conidia were tested for each conidial preparation in 3 independent experiments.

Extraction and quantification of conidial intracellular ATP. Conidial ATP extraction was carried out as described previously[73]. Briefly, freshly prepared extraction buffer (90% dimethylsulfoxide in Tris-acetate-EDTA) was heated to 100 °C for 2 min and mixed with an equal volume of ice-cold conidial suspension containing 1×10^7 conidia in 0.01% Tween 80. The mixture was further incubated at 100 °C for 1 min and then cooled on ice. The ATP assay was carried out within 2 h of extraction using the ATP Bioluminescent Assay Kit (catalogue no. FLAA; Sigma-Aldrich) according to the manufacturer's protocol.

Total protein extraction and western blot analysis. Trichloroacetic acid was used for total protein extraction as described previously[74] with the exception of the lysis step. Frozen conidia or press-dried hyphae were lysed in 500 µl of ice-cold denaturing buffer (10 mM of Tris-HCl, pH 8.0, 25 mM of NH_4 acetate, 1 mM of EDTA, 10% trichloroacetic acid) with approximately 100 µl volume of silica beads for 6 cycles of 3-min beating cycles using the Bullet Blender with 2 min of cooling on ice between each cycle. For membrane transporters, a modified resuspension buffer (0.1 M of Tris-HCl, pH 11.0, 3% of sodium dodecyl sulfate, 0.5% Triton X-100) was used to extract proteins from precipitated protein pellets by heating at 60 °C for 30 min. Total protein concentration was measured using the Bio-Rad *DC* Protein Assay Kit (catalogue no. 5000111; Bio-Rad Laboratories). The lysis efficiency of conidia collected at different developmental ages (that is, 3, 6 and 17 d after inoculation) were comparable as determined by the concentration of total protein extracts from the conidia preparations (Supplementary Fig. 3c). The same amounts of proteins from different samples were subjected to SDS–polyacrylamide gel electrophoresis and western blot analysis by Image Lab v5.2.1. Primary antibodies against haemagglutinin (1:2,000 dilution, catalogue no. sc-7392; Santa Cruz Biotechnology), Myc (1:2,000 dilution; catalogue no. sc-40; Santa Cruz Biotechnology), FLAG M2 (1:5,000 dilution, catalogue no. F3165; Sigma-Aldrich), histone H3 (1:5,000 dilution, catalogue no. ab1791; Abcam), HSP 70 (1:2,000 dilution, cat. no. sc-32239; Santa Cruz Biotechnology) and the horseradish peroxidase (HRP)-conjugated anti-rabbit (1:5,000 dilution, catalogue no. AP132P; Merck Millipore) and HRP-conjugated anti-mouse (1:5,000 dilution, catalogue no. AP124P; Merck Millipore) secondary antibodies were used.

***Galleria* infection assay.** A total of 2×10^5 conidia in 10 µl of PBS were injected into the last left proleg of a *Galleria mellonella* larva weighing about 0.3 g. Fifteen larvae were infected with each conidial preparation and different conidial preparations were assayed together in the same experiment. The infected worms were incubated at 30 °C and survival was monitored every 12 h. The survival rate was calculated from a total of at least 45 larvae from 3 independent experiments.

Sterigmatocystin extraction and analysis. The conidia of the *xylP*(p)*rsmA* strains were conidiated on solid ANM medium containing 1% glucose and 10 mM of ammonium tartrate with (pre-induced conidia) and without (non-induced conidia) 1% xylose for 2 d at 37 °C. The conidia (5×10^7) of the different preparations were grown in 100 ml of ANM medium containing 1% glucose, 1% xylose and 10 mM of ammonium tartrate at 37 °C with shaking at 220 r.p.m. for 4 d. For sterigmatocystin analysis, 10 ml of culture medium was taken on day 4 and mixed with 10 ml of ethyl acetate in an orbital shaker at 200 r.p.m. at 4 °C overnight. The aqueous fraction was recovered and dried by nitrogen gas

using the Eyela MGS-2200E Pressured Gas Blowing Concentrator. The dried powder was dissolved in 300 µl of ice-cold methanol and stored at −80 °C until ultra-performance liquid chromatography–mass spectrometry (UPLC–MS) analysis. For quantification, 2 µl of extract or sterigmatocystin reference standards (0.032 µg ml^{-1}, 0.16 µg ml^{-1}, 0.8 µg ml^{-1}, 4 µg ml^{-1} and 20 µg ml^{-1} dissolved in methanol; catalogue no. S3255; Sigma-Aldrich) was subjected to UPLC–MS analysis using an ACQUITY UPLC BEH C18 (1.7 µm, 2.1 × 100 mm) column on the Waters ACQUITY UPLC H-Class System. A gradient solvent analysis was carried out with a mobile phase of acetonitrile:water with 0.1% v/v formic acid at a flow rate of 0.4 ml min^{-1} with 6-min running time under the following conditions: the programme was initiated with 50% acetonitrile for 1 min, then increased to 90% for 3 min, to 95% for 1 min, returning to 50% within 0.1 min and balanced for another 0.9 min. Sterigmatocystin tandem mass spectrometry (MS/MS) detection was performed using pairs of ions at an *m/z* of 325.0/115.0 through a Waters Xevo TQD equipped with an electrospray ionization source in the positive ion mode. The capillary voltage was 4.0 kV. Nitrogen gas was flowed as the cone and desolvation gas at rates of 50 and 1,000 l h^{-1}, respectively. The source and desolvation temperatures were 200 and 500 °C, respectively. Cone and collision voltages were optimized to 8 and 68 V for sterigmatocystin with a dwell time of 25 ms. Data were processed with the Waters MassLynx V.4.1 software to calculate peak areas for quantification.

Gliotoxin extraction and analysis. For gliotoxin extraction from conidia, conidia grown on ANM medium containing 1% glucose and 10 mM of ammonium tartrate with or without zinc for 3 d were collected as described above. Approximately 0.5×10^{11} conidia were washed with 50 ml of ice-cold water three times to remove trace amounts of gliotoxin, if any, that might have come along through scraping conidia off the solid medium surface. Washed conidia were then lysed using 100 µl volume of silica beads for 8 cycles of 1-min beating using the Bullet Blender. Samples were cooled on ice for at least 1 min between each beating. The lysate was mixed with 4 ml of chloroform in an end-to-end rotator at 4 °C overnight. The aqueous phase was collected and dried by nitrogen gas using the Eyela MGS-2200E Pressured Gas Blowing Concentrator. The dried powder was dissolved in 500 µl of ice-cold methanol and stored at −80 °C until UPLC–MS analysis. Then, 60 µl of the extract was subjected to UPLC–MS analysis. For gliotoxin analysis in liquid growth medium, 1×10^8 control or zinc-starved conidia were grown in 100 ml of ANM medium containing 1% glucose and 10 mM of ammonium tartrate without zinc at 37 °C with shaking at 200 r.p.m. for 5 d. Every 24 h, 10 ml of medium was taken for extraction in the same way as described for sterigmatocystin, except that chloroform (instead of ethyl acetate) was used and the dried powder was dissolved in 300 µl of methanol. Extraction was performed on culture medium sampled after the indicated length of growth. For quantification, 2.5 µl of extract or freshly prepared gliotoxin reference standards (0.67 µg ml^{-1}, 2 µg ml^{-1}, 6 µg ml^{-1}, 18 µg ml^{-1}, 54 µg ml^{-1}, 162 µg ml^{-1} and 486 µg ml^{-1} dissolved in methanol; catalogue no. G9893; Sigma-Aldrich) was subjected to reverse-phase UPLC–MS analysis using an ACQUITY UPLC BEH C18 (1.7 µm, 2.1 × 100 mm) column on the Waters ACQUITY UPLC H-Class System. A gradient solvent analysis was carried out with a mobile phase of acetonitrile:water with 0.1% v/v ammonium hydroxide at a flow rate of 0.4 ml min^{-1} with 7-min running time under the following conditions: the programme was initiated with 30% acetonitrile for 1 min, then increased to 70% for 2 min, to 95% for 1 min, returning to 30% within 0.1 min and balanced for another 2.9 min. Gliotoxin MS/MS detection was carried out using pairs of ions at an *m/z* of 324.9/261.0 through a Waters Xevo TQD equipped with an electrospray ionization source in the negative ion mode. The capillary voltage was 4.0 kV. Nitrogen gas was employed as the cone and desolvation gas at flow rates of 50 and 1,000 l h^{-1}, respectively. The source and desolvation temperatures were 200 and 500 °C. Cone and collision voltages were optimized to 24 and 10 V for gliotoxin with a dwell time of 25 ms. Data were processed with the Waters MassLynx V.4.1 software to calculate peak areas for quantification.

Transcription inhibition test. We attempted to inhibit conidial transcriptional response using RNAP II inhibitors (α-amanitin, triptolide and actinomycin D) and found that these drugs were ineffective in *A. nidulans*[75] based on growth testing on solid medium (Supplementary Fig. 3d). The growth test was performed in a 96-well plate for a wild-type (WT) strain (CWF500) on ANM in the presence or absence (control) of the transcription inhibitor α-amanitin (5 µl (catalogue no. A2263; Sigma-Aldrich) into 150 µl of medium; approximately 28.75 µg ml^{-1}), actinomycin D (25 µg ml^{-1}; catalogue no. A1410; Sigma-Aldrich) or triptolide (25 µM; catalogue no. CAY11973; Cayman Chemical). These concentrations used are around 14–25 times higher than the recommended concentration for inhibiting transcription[76]. The translation inhibitor cycloheximide (2 mg ml^{-1}; catalogue no. C8500; United States Biological) was included as a control. Images were taken after growth at 37 °C for 24 h.

Statistics. Statistical analysis was performed using Prism 7.0 (GraphPad Software) and the statistical methods used are indicated in the legends of the relevant figures.

Reporting Summary. Further information on research design is available in the Nature Research Reporting Summary linked to this article.

Data availability

Next-generation sequencing data are available from the National Center for Biotechnology Information Sequence Read Archive database under accession no. PRJNA602418 for the RNAP II ChIP–seq data, PRJNA602550 for the TBP and TFIIB ChIP–seq data, PRJNA602580 for the RNAP I and RNAP III ChIP–seq data, PRJNA602549 for the histone modifications ChIP–seq data and PRJNA607649 for the RNA-seq data. A list of figures that have associated raw data is given in Supplementary Table 10. Gene annotation and GO information were obtained from AspGD (http://www.aspgd.org) and FungiDB (https://fungidb.org). Source data are provided with this paper.

Code availability

All scripts reported in the Methods are available at Github (https://github.com/zqmiao-mzq/closest_gene_calling/blob/master/zqWinSGR-v4.pl; https://github.com/zqmiao-mzq/closest_gene_calling/blob/master/closest_gene_calling_v10.pl; and https://github.com/sethiyap/FungalSporeAnalysis) or at the bioinformatics analysis platform FungiExpresZ (https://cparsania.shinyapps.io/FungiExpresZ/) (Chirag Parsania, unpublished).

Received: 4 June 2020; Accepted: 18 May 2021;
Published online: 28 June 2021

References

1. Lamarre, C. et al. Transcriptomic analysis of the exit from dormancy of *Aspergillus fumigatus* conidia. *BMC Genom.* **9**, 417 (2008).
2. Osherov, N. & May, G. S. The molecular mechanisms of conidial germination. *FEMS Microbiol. Lett.* **199**, 153–160 (2001).
3. Beuchat, L. R. Thermal tolerance of *Talaromyces flavus* ascospores as affected by growth medium and temperature, age and sugar content in the inactivation medium. *Trans. Brit. Mycol. Soc.* **90**, 359–364 (1988).
4. Blango, M. G. et al. Dynamic surface proteomes of allergenic fungal conidia. *J. Proteome Res.* **19**, 2092–2104 (2020).
5. Blaszyk, M., Blank, G., Holley, R. & Chong, J. Reduced water activity during sporogenesis in selected penicillia: impact on spore quality. *Food Res. Int.* **31**, 503–509 (1998).
6. Bleichrodt, R.-J., Foster, P., Howell, G., Latgé, J.-P. & Read, N. D. Cell wall composition heterogeneity between single cells in *Aspergillus fumigatus* leads to heterogeneous behavior during antifungal treatment and phagocytosis. *mBio* **11**, e03015-19 (2020).
7. Cliquet, S. & Jackson, M. Influence of culture conditions on production and freeze-drying tolerance of *Paecilomyces fumosoroseus* blastospores. *J. Ind. Microbiol. Biotechnol.* **23**, 97–102 (1999).
8. Cliquet, S. & Jackson, M. A. Impact of carbon and nitrogen nutrition on the quality, yield and composition of blastospores of the bioinsecticidal fungus *Paecilomyces fumosoroseus*. *J. Ind. Microbiol. Biotechnol.* **32**, 204–210 (2005).
9. Conner, D. E. & Beuchat, L. R. Efficacy of media for promoting ascospore formation by *Neosartorya fischeri*, and the influence of age and culture temperature on heat resistance of ascospores. *Food Microbiol.* **4**, 229–238 (1987).
10. Conner, D. E. & Beuchat, L. R. Heat resistance of ascospores of *Neosartorya fischeri* as affected by sporulation and heating medium. *Int. J. Food Microbiol.* **4**, 303–312 (1987).
11. Dagnas, S., Gougouli, M., Onno, B., Koutsoumanis, K. P. & Membre, J.-M. Quantifying the effect of water activity and storage temperature on single spore lag times of three moulds isolated from spoiled bakery products. *Int. J. Food Microbiol.* **240**, 75–84 (2017).
12. Darby, R. T. & Mandels, G. R. Effects of sporulation medium and age on fungus spore physiology. *Plant Physiol.* **30**, 360–366 (1955).
13. Hagiwara, D. et al. Temperature during conidiation affects stress tolerance, pigmentation, and trypacidin accumulation in the conidia of the airborne pathogen *Aspergillus fumigatus*. *PLoS ONE* **12**, e0177050 (2017).
14. Hallsworth, J. E. & Magan, N. Culture age, temperature, and pH affect the polyol and trehalose contents of fungal propagules. *Appl. Environ. Microbiol.* **62**, 2435–2442 (1996).
15. Jackson, M. A. & Schisler, D. A. The composition and attributes of *Colletotrichum truncatum* spores are altered by the nutritional environment. *Appl. Environ. Microbiol.* **58**, 2260–2265 (1992).
16. Kang, S. E., Celia, B., Bensasson, D. & Monamy, M. Sporulation environment drives phenotypic variation in the pathogen *Aspergillus fumigatus*. *G3 Genes Genom. Genet.* https://doi.org/10.1093/g3journal/jkab208 (2021).
17. Nguyen Van Long, N. et al. Temperature, water activity and pH during conidia production affect the physiological state and germination time of *Penicillium* species. *Int. J. Food Microbiol.* **241**, 151–160 (2017).
18. Oliveira, A. S., Braga, G. U. L. & Rangel, D. E. N. *Metarhizium robertsii* illuminated during mycelial growth produces conidia with increased germination speed and virulence. *Fungal Biol.* **122**, 555–562 (2018).
19. Oliveira, A. S. & Rangel, D. E. N. Transient anoxia during *Metarhizium robertsii* growth increases conidial virulence to *Tenebrio molitor*. *J. Invertebr. Pathol.* **153**, 130–133 (2018).

20. Oliveira, M., Pereira, C., Bessa, C., Araujo, R. & Saraiva, L. Chronological aging in conidia of pathogenic *Aspergillus*: comparison between species. *J. Microbiol. Methods* **118**, 57–63 (2015).
21. Teertstra, W. R. et al. Maturation of conidia on conidiophores of *Aspergillus niger*. *Fungal Genet. Biol.* **98**, 61–70 (2017).
22. Takahashi-Nakaguchi, A. et al. *Aspergillus fumigatus* adhesion factors in dormant conidia revealed through comparative phenotypic and transcriptomic analyses. *Cell Microbiol.* **20**, e12802 (2018).
23. Wösten, H. A., van Veluw, G. J., de Bekker, C. & Krijgsheld, P. Heterogeneity in the mycelium: implications for the use of fungi as cell factories. *Biotechnol. Lett.* **35**, 1155–1164 (2013).
24. Ackermann, M. A functional perspective on phenotypic heterogeneity in microorganisms. *Nat. Rev. Microbiol.* **13**, 497–508 (2015).
25. Avery, S. V. Microbial cell individuality and the underlying sources of heterogeneity. *Nat. Rev. Microbiol.* **4**, 577–587 (2006).
26. Hewitt, S. K., Foster, D. S., Dyer, P. S. & Avery, S. V. Phenotypic heterogeneity in fungi: importance and methodology. *Fungal Biol. Rev.* **30**, 176–184 (2016).
27. Kasuga, T. et al. Long-oligomer microarray profiling in *Neurospora crassa* reveals the transcriptional program underlying biochemical and physiological events of conidial germination. *Nucleic Acids Res.* **33**, 6469–6485 (2005).
28. van Leeuwen, M. R. et al. Germination of conidia of *Aspergillus niger* is accompanied by major changes in RNA profiles. *Stud. Mycol.* **74**, 59–70 (2013).
29. Novodvorska, M. et al. Trancriptional landscape of *Aspergillus niger* at breaking of conidial dormancy revealed by RNA-sequencing. *BMC Genom.* **14**, 246 (2013).
30. Zahiri, A. R., Babu, M. R. & Saville, B. J. Differential gene expression during teliospore germination in *Ustilago maydis*. *Mol. Genet. Genomics* **273**, 394–403 (2005).
31. Baltussen, T. J. H., Coolen, J. P. M., Zoll, J., Verweij, P. E. & Melchers, W. J. G. Gene co-expression analysis identifies gene clusters associated with isotropic and polarized growth in *Aspergillus fumigatus* conidia. *Fungal Genet. Biol.* **116**, 62–72 (2018).
32. Liu, T. et al. The use of global transcriptional analysis to reveal the biological and cellular events involved in distinct development phases of *Trichophyton rubrum* conidial germination. *BMC Genom.* **8**, 100 (2007).
33. Inglis, D. O., Voorhies, M., Hocking Murray, D. R. & Sil, A. Comparative transcriptomics of infectious spores from the fungal pathogen *Histoplasma capsulatum* reveals a core set of transcripts that specify infectious and pathogenic states. *Eukaryot. Cell* **12**, 828–852 (2013).
34. Hagiwara, D. et al. Comparative transcriptome analysis revealing dormant conidia and germination associated genes in *Aspergillus* species: an essential role for AtfA in conidial dormancy. *BMC Genom.* **17**, 358 (2016).
35. Taubitz, A., Bauer, B., Heesemann, J. & Ebel, F. Role of respiration in the germination process of the pathogenic mold *Aspergillus fumigatus*. *Curr. Microbiol.* **54**, 354–360 (2007).
36. Novodvorska, M. et al. Metabolic activity in dormant conidia of *Aspergillus niger* and developmental changes during conidial outgrowth. *Fungal Genet. Biol.* **94**, 23–31 (2016).
37. Osherov, N., Mathew, J., Romans, A. & May, G. S. Identification of conidial-enriched transcripts in *Aspergillus nidulans* using suppression subtractive hybridization. *Fungal Genet. Biol.* **37**, 197–204 (2002).
38. Lara-Rojas, F., Sánchez, O., Kawasaki, L. & Aguirre, J. *Aspergillus nidulans* transcription factor AtfA interacts with the MAPK SakA to regulate general stress responses, development and spore functions. *Mol. Microbiol.* **80**, 436–454 (2011).
39. Krijgsheld, P. et al. Development in *Aspergillus*. *Stud. Mycol.* **74**, 1–29 (2013).
40. Etxebeste, O., Garzia, A., Espeso, E. A. & Ugalde, U. *Aspergillus nidulans* asexual development: making the most of cellular modules. *Trends Microbiol.* **18**, 569–576 (2010).
41. Momany, M., Zhao, J., Lindsey, R. & Westfall, P. J. Characterization of the *Aspergillus nidulans* septin (*asp*) gene family. *Genetics* **157**, 969–977 (2001).
42. Oakley, B. R. Tubulins in *Aspergillus nidulans*. *Fungal Genet. Biol.* **41**, 420–427 (2004).
43. Petrenko, N., Jin, Y., Dong, L., Wong, K. H. & Struhl, K. Requirements for RNA polymerase II preinitiation complex formation in vivo. *eLife* **8**, e43654 (2019).
44. Moreno, M. A. et al. The regulation of zinc homeostasis by the ZafA transcriptional activator is essential for *Aspergillus fumigatus* virulence. *Mol. Microbiol.* **64**, 1182–1197 (2007).
45. Champe, S. P., Rao, P. & Chang, A. An endogenous inducer of sexual development in *Aspergillus nidulans*. *J. Gen. Microbiol.* **133**, 1383–1387 (1987).
46. Teutschbein, J. et al. Proteome profiling and functional classification of intracellular proteins from conidia of the human-pathogenic mold *Aspergillus fumigatus*. *J. Proteome Res.* **9**, 3427–3442 (2010).
47. Wu, M.-Y. et al. Systematic dissection of the evolutionarily conserved WetA developmental regulator across a genus of filamentous fungi. *mBio* **9**, e01130-18 (2018).
48. Anjo, S. I., Figueiredo, F., Fernandes, R., Manadas, B. & Oliveira, M. A proteomic and ultrastructural characterization of *Aspergillus fumigatus*' conidia adaptation at different culture ages. *J. Proteomics* **161**, 47–56 (2017).
49. Doyle, M. P. & Marth, E. H. Thermal inactivation of conidia from *Aspergillus flavus* and *Aspergillus parasiticus*. I. Effects of moist heat, age of conidia, and sporulation medium. *J. Milk Food Technol.* **38**, 678–682 (1975).
50. Low, S. Y., Dannemiller, K., Yao, M., Yamamoto, N. & Peccia, J. The allergenicity of *Aspergillus fumigatus* conidia is influenced by growth temperature. *Fungal Biol.* **115**, 625–632 (2011).
51. Arias, M. et al. Preparations for invasion: modulation of host lung immunity during pulmonary *Aspergillosis* by gliotoxin and other fungal secondary metabolites. *Front. Immunol.* **9**, 2549 (2018).
52. Bok, J. W. et al. GliZ, a transcriptional regulator of gliotoxin biosynthesis, contributes to *Aspergillus fumigatus* virulence. *Infect. Immun.* **74**, 6761–6768 (2006).
53. Houšť, J., Spížek, J. & Havlíček, V. Antifungal drugs. *Metabolites.* **10**, 106 (2020).
54. Bignell, E., Cairns, T. C., Throckmorton, K., Nierman, W. C. & Keller, N. P. Secondary metabolite arsenal of an opportunistic pathogenic fungus. *Philos. Trans. R. Soc. Lond. B Biol. Sci.* **371**, 20160023 (2016).
55. Fernandes, M., Keller, N. P. & Adams, T. H. Sequence-specific binding by *Aspergillus nidulans* AflR, a C6 zinc cluster protein regulating mycotoxin biosynthesis. *Mol. Microbiol.* **28**, 1355–1365 (1998).
56. Zadra, I., Abt, B., Parson, W. & Haas, H. *xylP* promoter-based expression system and its use for antisense downregulation of the *Penicillium chrysogenum* nitrogen regulator NRE. *Appl. Environ. Microbiol.* **66**, 4810–4816 (2000).
57. Shaaban, M. I., Bok, J. W., Lauer, C. & Keller, N. P. Suppressor mutagenesis identifies a velvet complex remediator of *Aspergillus nidulans* secondary metabolism. *Eukaryot. Cell* **9**, 1816–1824 (2010).
58. Baltussen, T. J. H., Zoll, J., Verweij, P. E. & Melchers, W. J. G. Molecular mechanisms of conidial germination in *Aspergillus* spp. *Microbiol. Mol. Biol. Rev.* **84**, e00049-19 (2019).
59. Money, N. P. in *The Fungi* (eds Watkinson, S. C. et al.) 67–97 (Academic Press, 2016).
60. Qin, L. et al. Universal plasmids to facilitate gene deletion and gene tagging in filamentous fungi. *Fungal Genet. Biol.* **125**, 28–35 (2019).
61. Todd, R. B., Davis, M. A. & Hynes, M. J. Genetic manipulation of *Aspergillus nidulans*: heterokaryons and diploids for dominance, complementation and haploidization analyses. *Nat. Protoc.* **2**, 822–830 (2007).
62. Fan, X., Lamarre-Vincent, N., Wang, Q. & Struhl, K. Extensive chromatin fragmentation improves enrichment of protein binding sites in chromatin immunoprecipitation experiments. *Nucleic Acids Res.* **36**, e125 (2008).
63. Wong, K. H. & Struhl, K. The Cyc8–Tup1 complex inhibits transcription primarily by masking the activation domain of the recruiting protein. *Genes Dev.* **25**, 2525–2539 (2011).
64. Wong, K. H., Jin, Y. & Moqtaderi, Z. Multiplex Illumina sequencing using DNA barcoding. *Curr. Protoc. Mol. Biol.* **101**, 7.11.1–7.11.11 (2013).
65. Rio, D. C., Ares, M.Jr., Hannon, G. J. & Nilsen, T. W. Purification of RNA using TRIzol (TRI reagent). *Cold Spring Harb. Protoc.* **6**, pdb-prot5439 (2010).
66. Langmead, B., Trapnell, C., Pop, M. & Salzberg, S. L. Ultrafast and memory-efficient alignment of short DNA sequences to the human genome. *Genome Biol.* **10**, R25 (2009).
67. Zhang, Y. et al. Model-based analysis of ChIP–Seq (MACS). *Genome Biol.* **9**, R137 (2008).
68. Pertea, M., Kim, D., Pertea, G. M., Leek, J. T. & Salzberg, S. L. Transcript-level expression analysis of RNA-seq experiments with HISAT, StringTie and Ballgown. *Nat. Protoc.* **11**, 1650–1667 (2016).
69. Ashburner, M. et al. Gene Ontology: tool for the unification of biology. *Nat. Genet.* **25**, 25–29 (2000).
70. Stajich, J. E. et al. FungiDB: an integrated functional genomics database for fungi. *Nucleic Acids Res.* **40**, D675–D681 (2012).
71. Rueden, C. T. et al. ImageJ2: ImageJ for the next generation of scientific image data. *BMC Bioinform.* **18**, 529 (2017).
72. Maleszka, R. & Pieniazek, N. J. Modified replica plating technique of microcolonies of *Aspergillus nidulans* using Triton-X100. *Asp. Newsl.* **15**, 36–38 (1981).
73. Rakotonirainy, M. S., Héraud, C. & Lavédrine, B. Detection of viable fungal spores contaminant on documents and rapid control of the effectiveness of an ethylene oxide disinfection using ATP assay. *Luminescence* **18**, 113–121 (2003).
74. Wong, K. H., Hynes, M. J., Todd, R. B. & Davis, M. A. Transcriptional control of *nmrA* by the bZIP transcription factor MeaB reveals a new level of nitrogen regulation in *Aspergillus nidulans*. *Mol. Microbiol.* **66**, 534–551 (2007).
75. Stunnenberg, H. G., Wennekes, L. M., Spierings, T. & van den Broek, H. W. An alpha-amanitin-resistant DNA-dependent RNA polymerase II from the fungus *Aspergillus nidulans*. *Eur. J. Biochem.* **117**, 121–129 (1981).
76. Bensaude, O. Inhibiting eukaryotic transcription: which compound to choose? How to evaluate its activity? *Transcription* **2**, 103–108 (2011).

Acknowledgements

We thank members of the Wong laboratory for comments and discussions throughout the study and M. J. Hynes, A. Andrianopoulos, R. B. Todd, M. Momany and K. Struhl for insightful discussions. We acknowledge the services and technical supports from the Genomics and Single Cell Analysis Core and the Drug and Development Core of the Faculty of Health Sciences at the University of Macau. This work was performed in part at the High-Performance Computing Cluster (HPC), which is supported by the Information and Communication Technology Office (ICTO) of the University of Macau. We thank L. Pardeshi and N. Shirgaonkar from the Genomics, Bioinformatics and Single Cell Analysis Core and Z. Miao and C. Parsania for Bioinformatics support, and J. Chan from ICTO for technical support on the HPC. We also acknowledge the support from the Science and Technology Development Fund, Macao S.A.R (FDCT) (project no. 0106/2020/A), the Research Services and Knowledge Transfer Office (project nos. MYRG2018-00017-FHS and MYRG2019-00099-FHS) and Faculty of Health Sciences of the University of Macau to K.H.W.

Author contributions

F.W. and K.H.W. conceived the study, designed the experiments and interpreted the data. F.W. performed the experiments. F.W. performed the bioinformatics analysis with help from P.S. K.T. performed the Illumina sequencing and provided technical support. F.W. and X.H. performed the LC–MS analysis. F.W., S.G., Y.C. and A.L. engineered the strains. K.H.W. provided the funding. F.W. and K.H.W. wrote the manuscript.

Competing interests

The authors declare no competing interests.

Additional information

Extended data is available for this paper at https://doi.org/10.1038/s41564-021-00922-y.

Supplementary information The online version contains supplementary material available at https://doi.org/10.1038/s41564-021-00922-y.

Correspondence and requests for materials should be addressed to K.H.W.

Peer review information *Nature Microbiology* thanks Jan Dijksterhuis, Jean-Paul Latge and the other, anonymous, reviewer(s) for their contribution to the peer review of this work. Peer reviewer reports are available.

Reprints and permissions information is available at www.nature.com/reprints.

Publisher's note Springer Nature remains neutral with regard to jurisdictional claims in published maps and institutional affiliations.

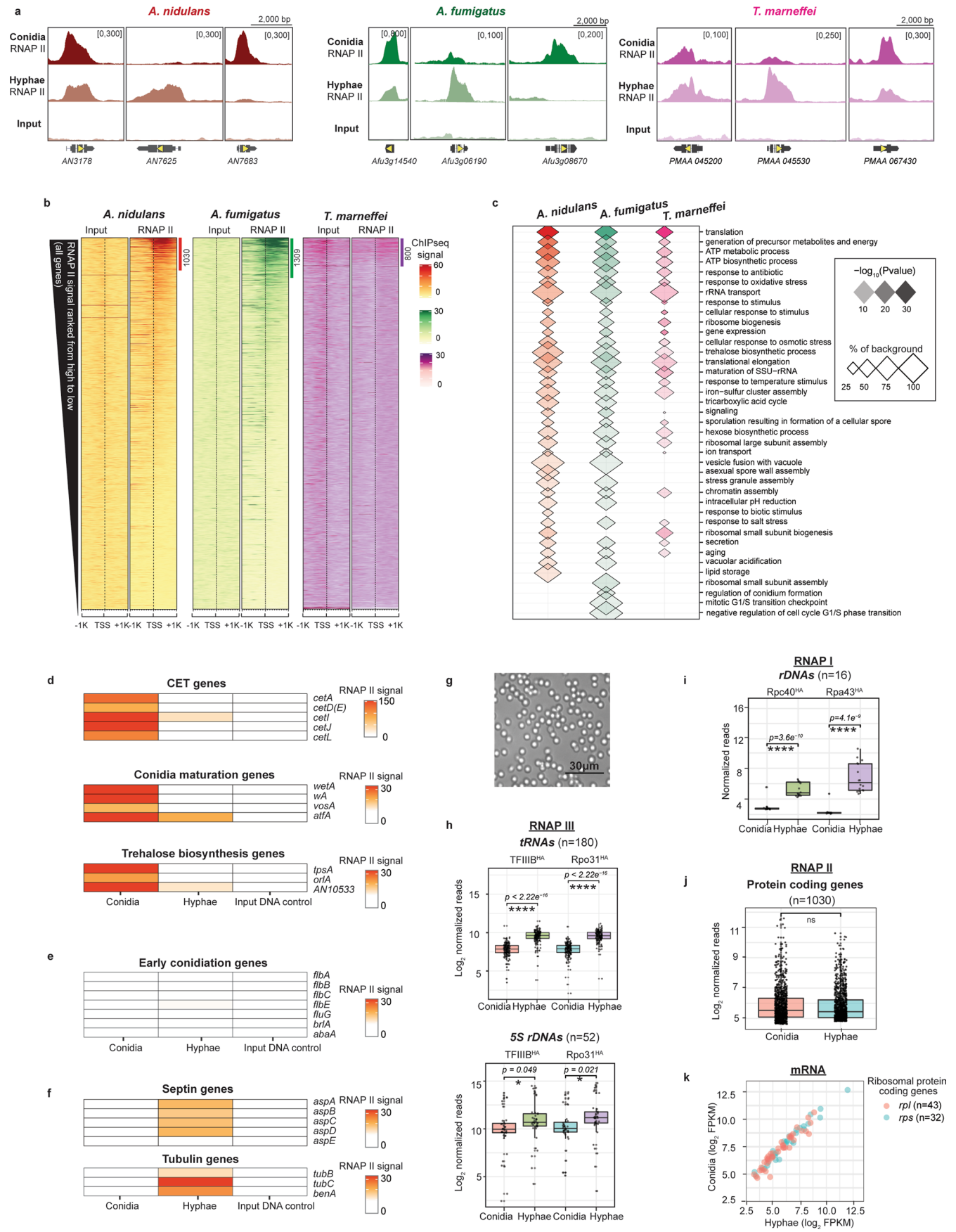

Extended Data Fig. 1 | See next page for caption.

Extended Data Fig. 1 | Conidia on conidiophore have robust transcription activities. a, Genome browser screenshots showing RNAP II ChIPseq and input DNA signals at selected genes with differential RNAP II occupancies for conidia and hyphae of *A. nidulans*, *A. fumigatus* and *T. marneffei*. **b**, Heatmap plots of RNAP II ChIPseq and input DNA signals at all annotated genes for conidia of the three species. The number of RNAP II occupied genes for each species is indicated on the colour lines at the right. **c**, A schematic diagram showing statistically significant (p-value < 0.01) GO terms enriched among transcribed genes for the three species. Colour intensity and size of diamonds indicate p-value and percentage of background, respectively. The p-value was calculated by Fisher's Exact test and was corrected for multiple testing using Benjamini-Hochberg false discovery rate and the Bonferroni method. **d**-**f**, Heatmap plots showing RNAP II ChIPseq signal at (**d**) conidia-enriched-transcripts (CET), conidial maturation and trehalose biosynthesis genes, (**e**) conidiation initiation genes, and (**f**) septin and β-tubulin genes for *A. nidulans* conidia and hyphae. Input DNA signals for conidia were included as a negative control. **g**, A representative microscopy image example for a conidial preparation of *A. nidulans* for ChIPseq and other experiments. The experiment was repeated three independent times with similar results, and representative image was presented. h-j, Boxplots showing (**h**) RNAP III ($TFIIIB^{HA}$ and $Rpo31^{HA}$), (**i**) RNAP I ($Rpc40^{HA}$ and $Rpa43^{HA}$) and (**j**) RNAP II binding signals at (**h**) tRNAs (n = 180) and 5 S rDNAs (n = 52), (**i**) rDNAs (n = 16) and (**j**) protein encoding genes (n = 1,030) in *A. nidulans* conidia and hyphae. Lower and upper hinges of boxes represent 25^{th} and 75^{th} percentiles, respectively, and the centre of boxes represents the median. The p-values shown were calculated using two samples t-test by ggplot2. The asterisks *, **, *** and **** depict p-values of <0.05, <0.005, <0.001 and <0.0001, respectively, while ns represents a p-value of >0.05. **k**, A scatter plot showing the comparable mRNA levels of ribosomal protein genes detected by RNAseq in conidia and hyphae.

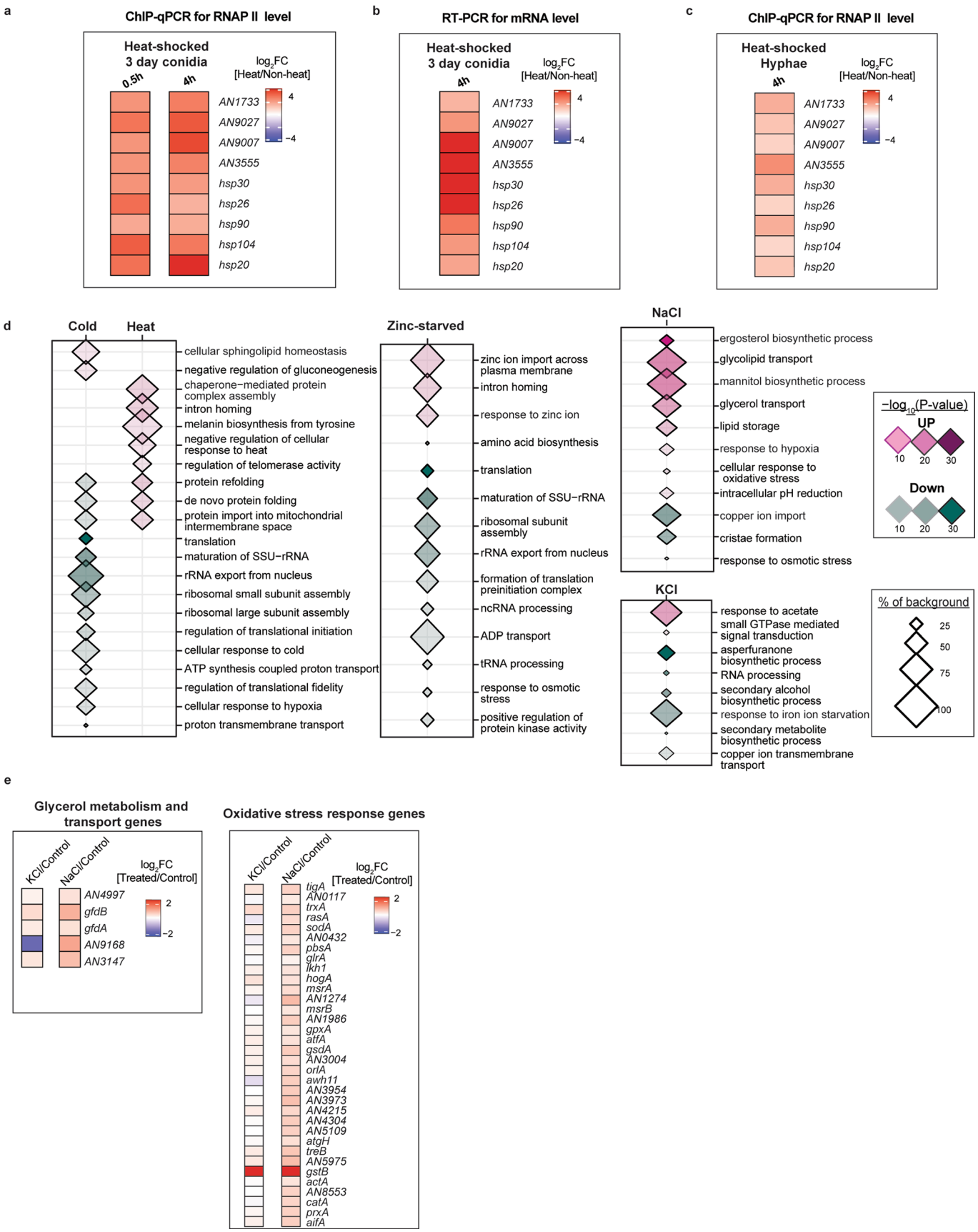

Extended Data Fig. 2 | See next page for caption.

Extended Data Fig. 2 | *A. nidulans* conidia transcriptionally respond to the environment, activating condition-specific physiological pathways. a-**b**, Heatbox plots showing (**a**) RNAP II binding and (**b**) mRNA levels of heat-shock response genes in conidia subjected to heat (42 °C) for 0.5 or 4 h as measured by (**a**) ChIP-qPCR and (**b**) RT-PCR, respectively. **c**, A heatbox plot showing RNAP II binding level as measured by ChIP-qPCR of heat shock response genes in hyphae after heat-shock treatment (4 h). **d**, Schematic diagrams showing GO analysis of differentially transcribed genes for *A. nidulans* conidia subjected to temperature shocks (4 and 42 °C) and control conidia (37 °C) or between *A. nidulans* conidia grown in the presence of sodium chloride (NaCl) or potassium chloride (KCl) or in the absence of zinc (Zinc-starved) comparing to control conidia from ANM media. Colour intensity and size of diamonds represent p-value (expressed as $-\log_{10}$p-value) and percentage of background. The p-value was calculated by Fisher's Exact test and was corrected for multiple testing using Benjamini-Hochberg false discovery rate and the Bonferroni method. **e**, Heatbox plots showing the RNAP II binding level of glycerol transport and oxidative stress response genes in NaCl and KCl conidia compared to Control conidia.

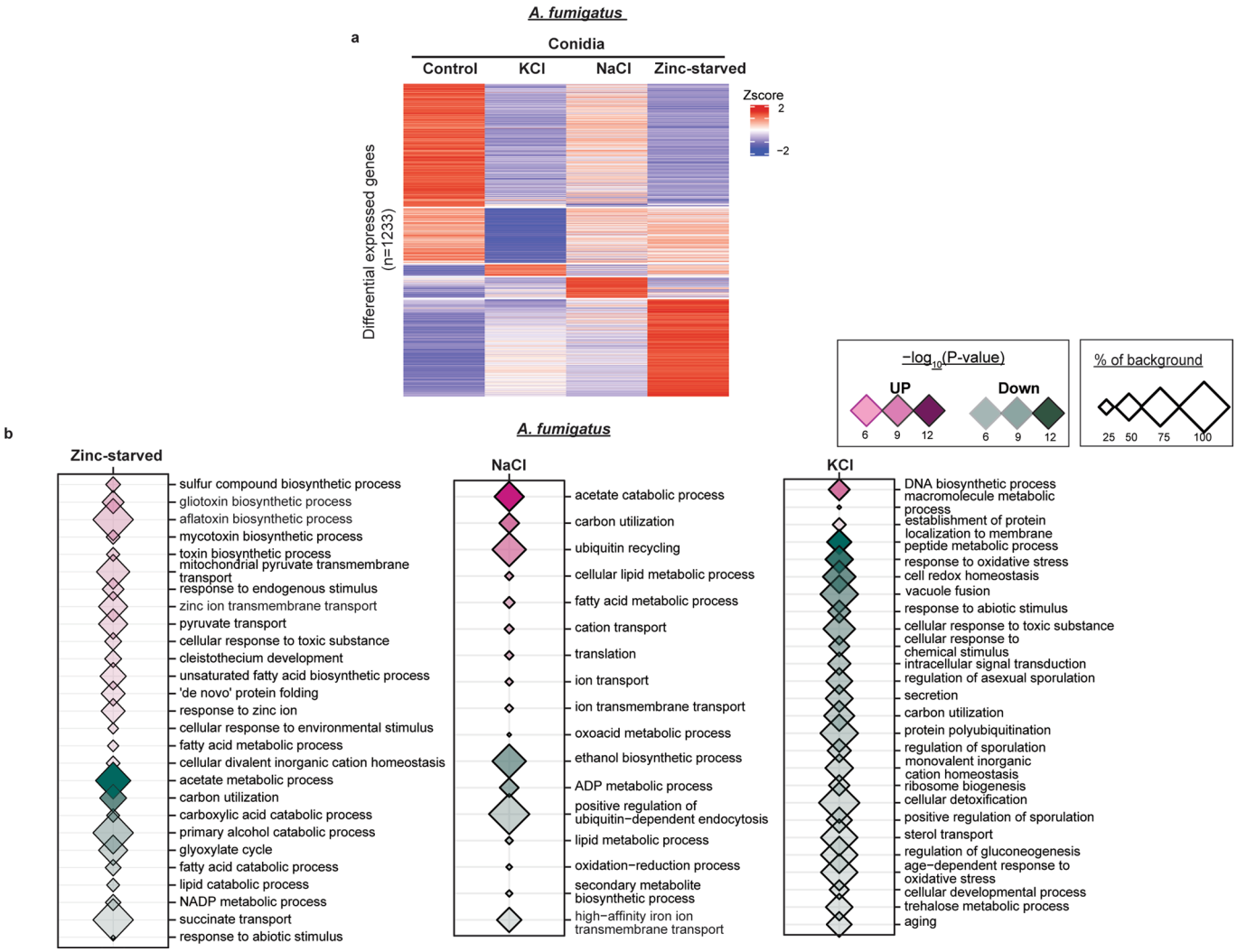

Extended Data Fig. 3 | *A. fumigatus* conidia transcriptionally respond to the environment, activating condition-specific physiological pathways. a, A heatmap plot showing differential expressed genes (presented as z-scores) among *A. fumigatus* conidia formed from ANM media in the presence of sodium chloride (NaCl) and potassium chloride (KCl) or in the absence of zinc (Zinc-starved). **b**, Schematic diagrams showing gene ontology analysis of differentially transcribed genes for *A. fumigatus* conidia grown in the presence of sodium chloride (NaCl) or potassium chloride (KCl) or in the absence of zinc (Zinc-starved), as compared to control conidia from ANM media. Colour intensity and size of diamonds represent p-value (expressed as $-\log_{10}$p-value) and percentage of background. The p-value was calculated by Fisher's Exact test and was corrected for multiple testing using Benjamini-Hochberg false discovery rate and the Bonferroni method.

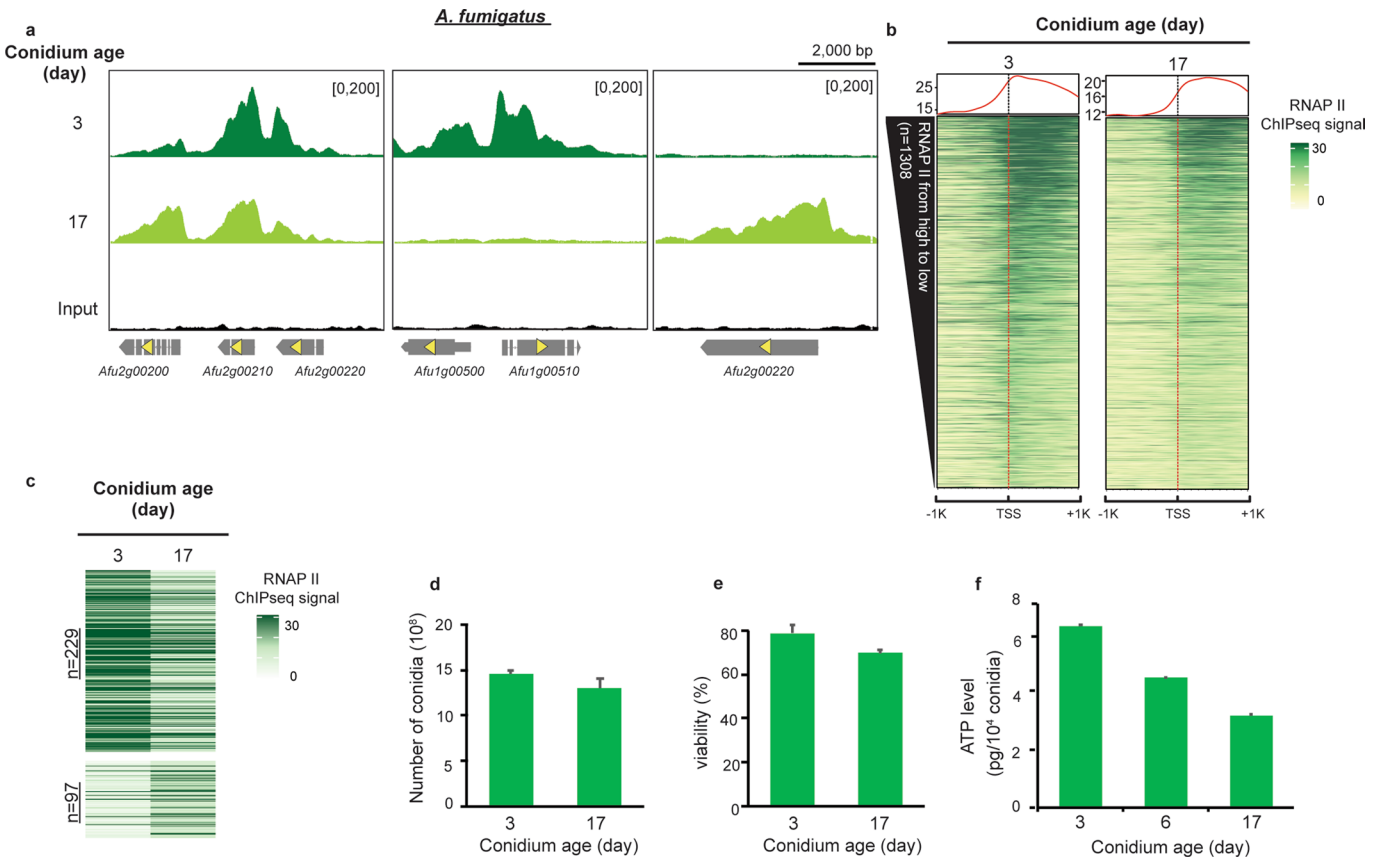

Extended Data Fig. 4 | *A. fumigatus* conidia have transcription and ATP-consuming activities even after conidial development has completed. a, Genome browser screenshots showing RNAP II ChIPseq and input DNA signals at selected genes with differential RNAP II occupancies for 3 and 17 day-old conidia. **b**, Heatmap plots showing RNAP II ChIPseq signals at genes occupied by RNAP II in either 3 or 17 day-old conidia. **c**, Heatmap plot showing differential expressed genes between 3 or 17 day-old conidia. **d**-**f**, Bar plots showing (**d**) the number of conidia, (**e**) viability and (**f**) intracellular ATP levels for conidia of different developmental ages (3, 6 or 17 day-old). **d**-**f** Data are presented as mean values + SD. Error bars represent the SD of three independent experiments (n = 3).

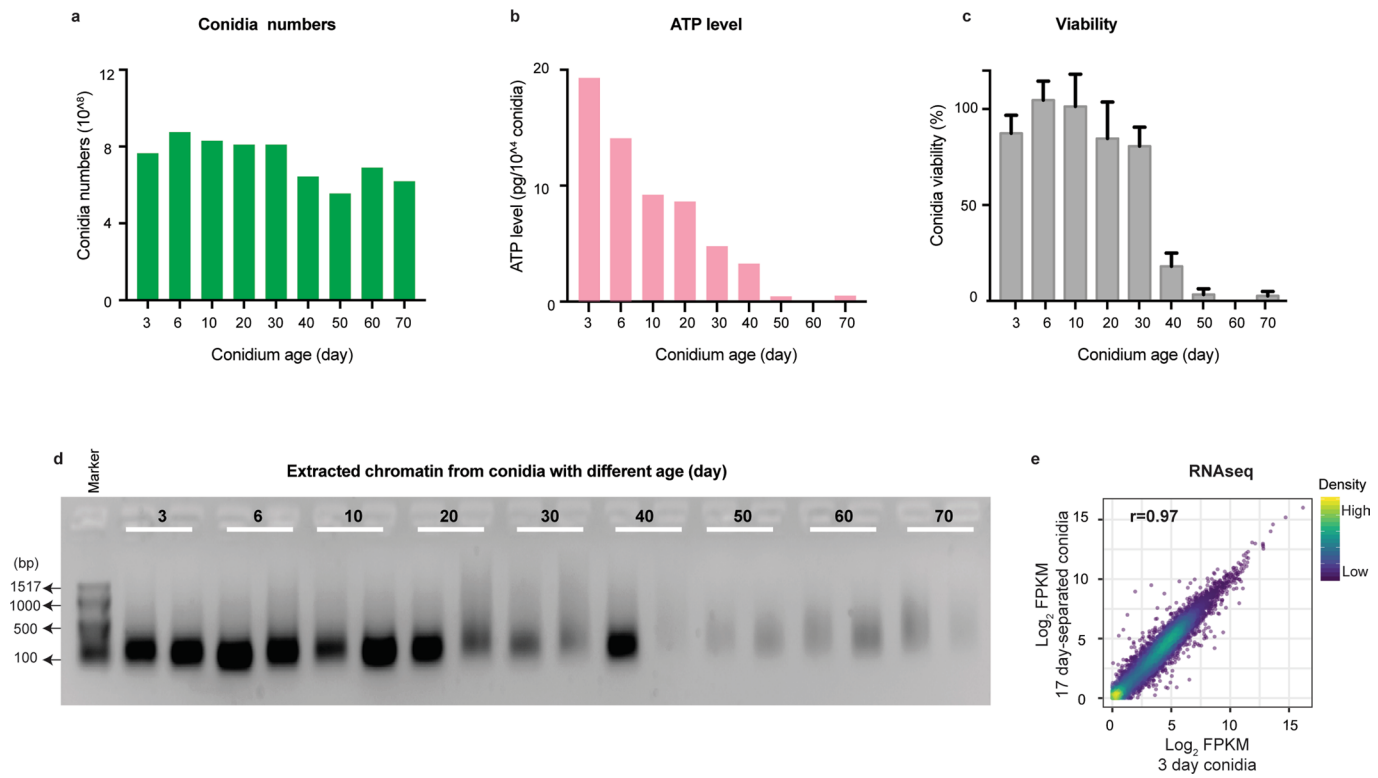

Extended Data Fig. 5 | Conidial ATP level is linked to conidial viability in *A. nidulans*. **a**-**b**, Bar graphs showing the mean (**a**) conidia numbers and (**b**) intracellular conidial ATP levels after the indicated time (that is, developmental age of conidia; 3, 6, 10, 20, 30, 40, 50, 60 and 70 day after inoculation) from two independent experiments. The same trend was observed in the biological repeats and the raw data are presented in Source Data Extended Data Fig. 5. **c**, A bar graph showing the viability of conidia same as (**a**-**b**). Data are presented as mean values + SD. Error bars represent the standard deviation of three independent experiments (n = 3). **d**, A gel electrophoresis result showing the quality and yield of chromatin extracted from conidia of different developmental ages collected in parallel with those conidia analyzed for **a**-**c**. **e**, A scatter plot showing the Pearson Correlation analysis of mRNA levels measured by RNAseq in attached and separated conidia as in Fig. 3h.

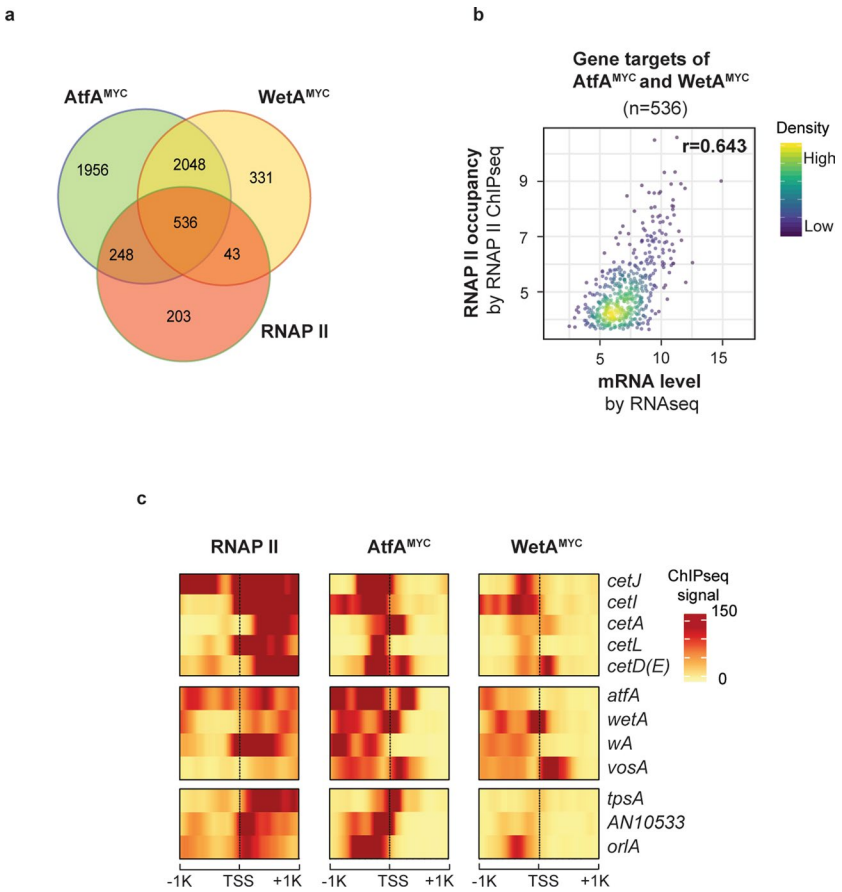

Extended Data Fig. 6 | Overlaps between RNAP II bound genes and targets of AtfA and WetA in *A. nidulans* conidia. a, A Venn diagram showing the overlap of genes occupied by RNAP II in conidia and binding targets (by ChIPseq) of transcription factor AtfA^{MYC} and WetA^{MYC} in conidia. **b**, A scatter plot showing Pearson Correlation of RNAP II occupancies and mRNA levels for AtfA and WetA common ChIPseq binding targets (n = 536) in conidia. **c**, Heatmap plots showing ChIPseq signals of RNAP II, WetA^{MYC} and AtfA^{MYC} for selected conidium-specific genes in *A. nidulans*.

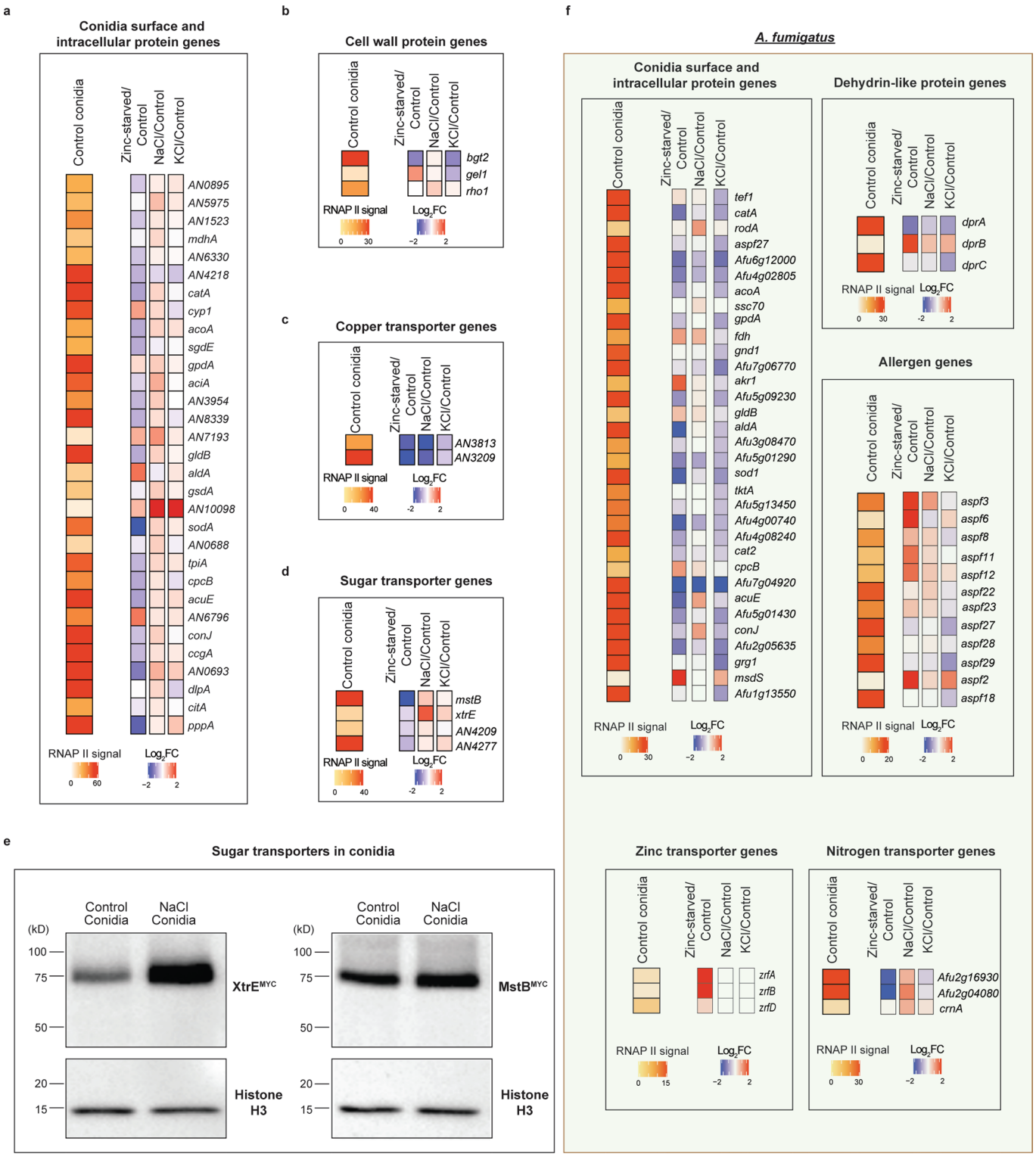

Extended Data Fig. 7 | *A. nidulans* and *A. fumigatus* conidia formed from different conditions have dissimilar transcriptional response and protein expression patterns. a-**d**, Heatbox plots showing RNAP II ChIPseq signals for genes encoding (**a**) conidia surface and intracellular proteins, (**b**) cell wall proteins, (**c**) copper and (**d**) sugar transporters in *A. nidulans* conidia formed under zinc deficiency (Zinc-starved conidia) or in the presence or absence (Control conidia) of NaCl and KCl (NaCl- and KCl-conidia, respectively). **e**, Western blot analysis showing the protein expression level of sugar transporters (for example XtrE and MstB) in control and NaCl conidia of *A. nidulans*. Histone H3 was used as a loading control. The Western blot experiment was repeated three independent times with similar result. **f**, Heatbox plots showing RNAP II ChIPseq signals for genes encoding conidia surface and intracellular proteins, dehydrin-like proteins, allergens and transporters in *A. fumigatus* conidia formed under zinc deficiency (Zinc-starved conidia) or in the presence or absence (Control conidia) of NaCl and KCl (NaCl- and KCl-conidia, respectively). Results of *A. fumigatus* are marked by green-shaded background.

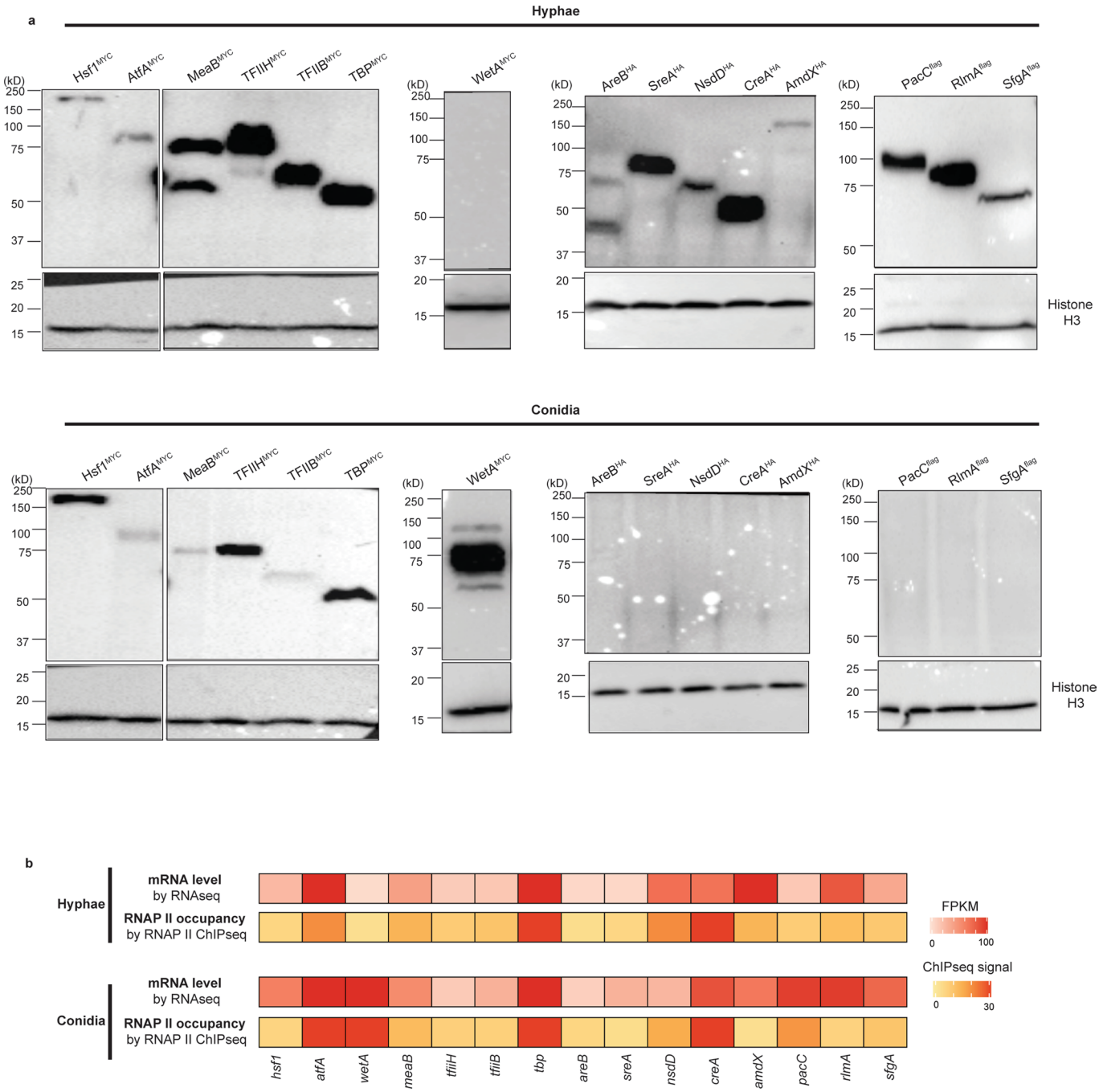

Extended Data Fig. 8 | Disparities between transcription, mRNA and protein levels in *A. nidulans* conidia. a, Western Blotting results showing protein levels of representative genes in *A. nidulans* conidia and hyphae. The Western blot experiment was repeated three independent times with similar result. **b**, Heatbox plots showing RNAP II ChIPseq and mRNA levels for the genes encoding those proteins analysed in (**a**) in conidia and hyphae.

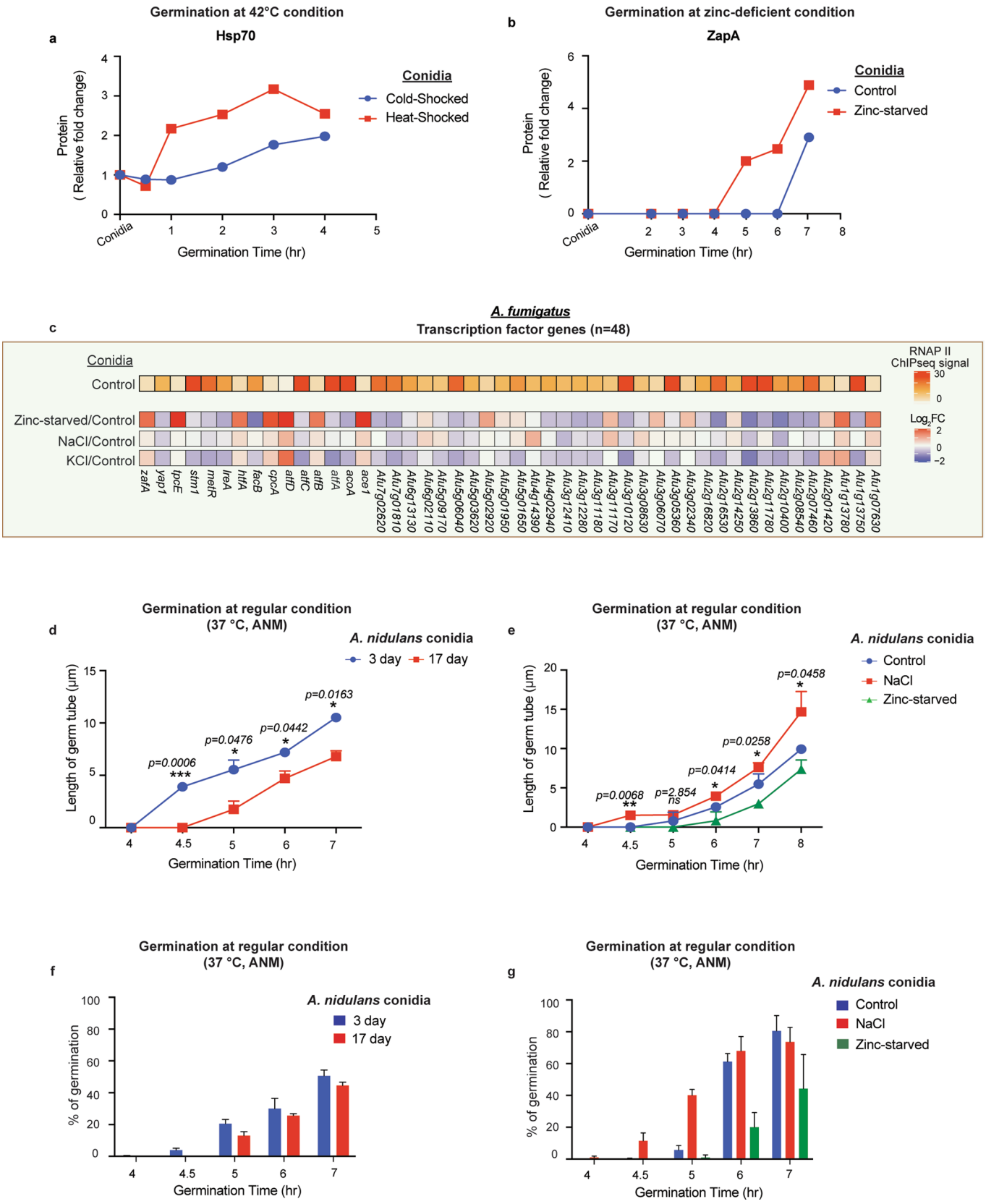

Extended Data Fig. 9 | See next page for caption.

Extended Data Fig. 9 | Sporulation conditions and conidial age affect the transcription levels of transcription factor-encoding genes, protein expression efficiency following germination and germination behaviours of *A. nidulans* and *A. fumigatus* conidia. a-**b**, Line plots showing the quantification of protein bands in the Western Blotting time-course analysis presented in Fig. 4f and g for (**a**) Hsp70 protein in heat-shocked and cold-shocked conidia during germination at high temperature (for example 42 °C) and (**b**) ZapA protein in control and zinc-starved conidia before and during germination in the absence of zinc. Histone H3 was used as a loading control. **c**, A heatbox plot showing the transcription levels for 48 transcription factor (TF)-encoding genes, which have detectable RNAP II ChIPseq signals, in Zinc-starved, NaCl-, KCl- and Control conidia of *A. fumigatus*. **d**-**e**, Line plots showing the germination kinetics of *A. nidulans* (**d**) conidia of different developmental ages (3 and 17 day-old) and (**e**) conidia formed under ANM media (Control) in the presence of sodium chloride (NaCl) or in the absence of zinc (Zinc-starved). Error bars represent the standard deviation of three independent experiments. The p-values shown were calculated using (**d**) unpaired t-test in two-tailed or (**e**) one way ANOVA with multiple comparisons test. **f**-**g**, Bar plots showing percentage of germination for *A. nidulans* conidia formed under the indicated conditions as in (**f**) and (**g**) at various germination times (for example 4 h, 4.5 h, 5 h, 6 h and 7 h). **d**-**g**, Data are presented as mean values + SD. Error bars represent the SD of three independent experiments (n = 3). The asterisks *, **, *** and **** depict p-values of <0.05, <0.005, <0.001 and <0.0001, respectively, while ns represents a p-value of >0.05. Results of *A. fumigatus* are marked by green-shaded background.

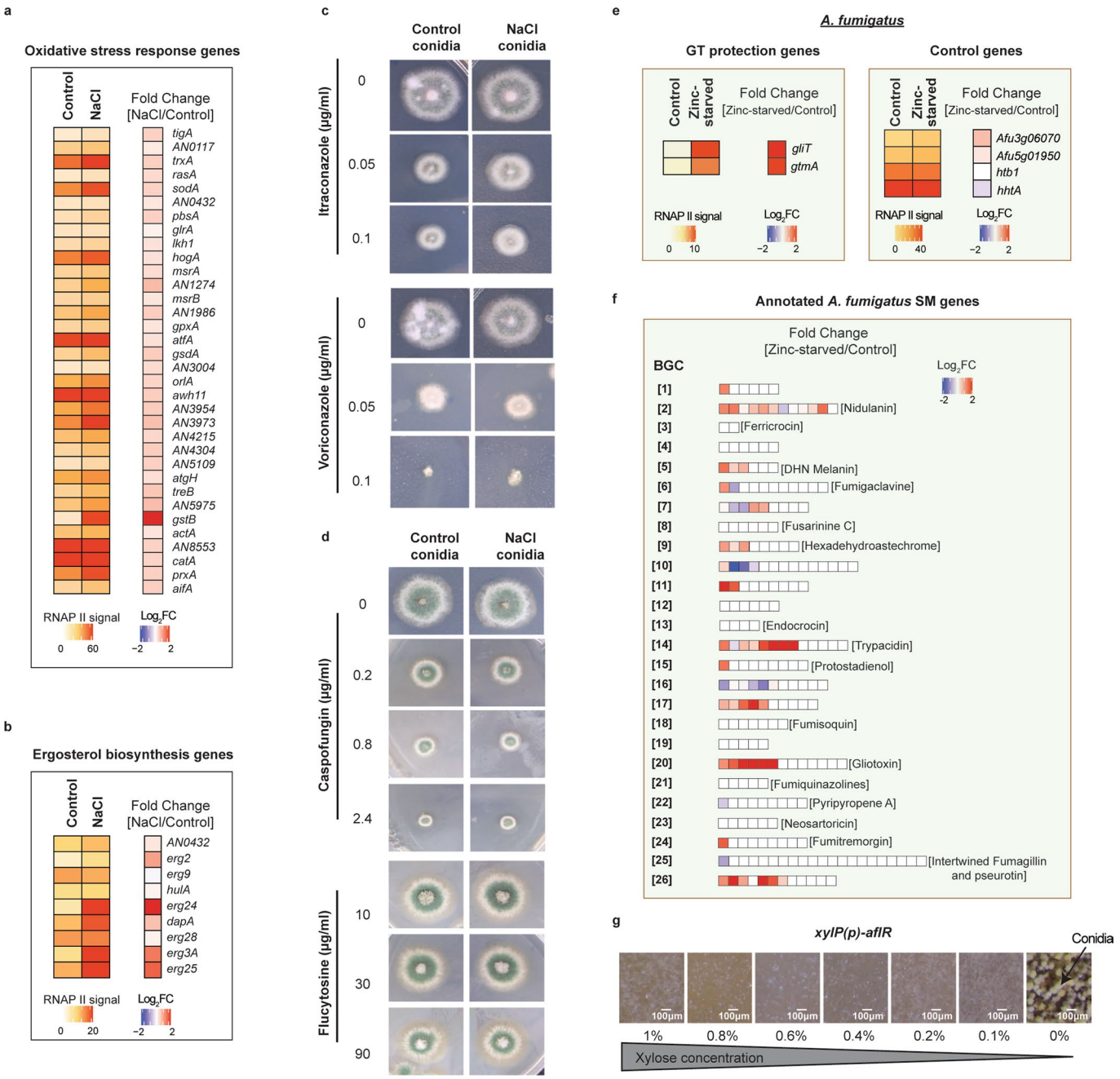

Extended Data Fig. 10 | Conidia formed under different sporulation conditions have different transcription levels for genes of various physiological pathways. a-**b**, Heatbox plots showing RNAP II ChIPseq signals and expression changes of (**a**) oxidative stress response genes and (**b**) ergosterol biosynthesis genes for *A. nidulans* conidia formed under ANM media (Control) and ANM media with sodium chloride (NaCl). **c**-**d**, Growth tests of *A. nidulans* wildtype strains on solid ANM media containing different concentrations of the azole-related anti-fungal drugs (**c**) itraconazole (0, 0.05 and 0.1 μg/ml) and voriconazole (0, 0.05 and 0.1 μg/ml), and the non-azole-related anti-fungal drugs (**d**) caspofungin (0.2, 0.8 and 2.4 μg/ml) and flucytosine (10, 30 and 90 μg/ml) using conidia formed under ANM media containing sodium chloride (NaCl conidia) or not (Control conidia). **e**, Heatbox plots showing RNAP II ChIPseq signals and expression changes of gliotoxin protection and control genes for *A. fumigatus* conidia formed on ANM media with (Control) and without zinc (Zinc-starved). **f**, Heatbox plots showing expression difference of annotated secondary metabolite biosynthesis clusters genes in *A. fumigatus* between conidia formed under ANM media with (Control) and without zinc (Zinc-starved). **g**, Microscopy images showing the conidiation phenotype of the *xylP*(p)*aflR* strain with different levels of xylose induction (0, 0.1, 0.2, 0.4, 0.6, 0.8 and 1%). Results of *A. fumigatus* are marked by green-shaded background. The experiment was performed three independent times with similar results and representative images are presented.

nature research

Corresponding author(s): Koon Ho Wong

Last updated by author(s): Jun 10, 2021

Reporting Summary

Nature Research wishes to improve the reproducibility of the work that we publish. This form provides structure for consistency and transparency in reporting. For further information on Nature Research policies, see our Editorial Policies and the Editorial Policy Checklist.

Statistics

For all statistical analyses, confirm that the following items are present in the figure legend, table legend, main text, or Methods section.

n/a	Confirmed	
☒	☐	The exact sample size (*n*) for each experimental group/condition, given as a discrete number and unit of measurement
☐	☒	A statement on whether measurements were taken from distinct samples or whether the same sample was measured repeatedly
☐	☒	The statistical test(s) used AND whether they are one- or two-sided *Only common tests should be described solely by name; describe more complex techniques in the Methods section.*
☒	☐	A description of all covariates tested
☒	☐	A description of any assumptions or corrections, such as tests of normality and adjustment for multiple comparisons
☐	☒	A full description of the statistical parameters including central tendency (e.g. means) or other basic estimates (e.g. regression coefficient) AND variation (e.g. standard deviation) or associated estimates of uncertainty (e.g. confidence intervals)
☐	☒	For null hypothesis testing, the test statistic (e.g. *F*, *t*, *r*) with confidence intervals, effect sizes, degrees of freedom and *P* value noted *Give P values as exact values whenever suitable.*
☒	☐	For Bayesian analysis, information on the choice of priors and Markov chain Monte Carlo settings
☒	☐	For hierarchical and complex designs, identification of the appropriate level for tests and full reporting of outcomes
☐	☒	Estimates of effect sizes (e.g. Cohen's *d*, Pearson's *r*), indicating how they were calculated

Our web collection on statistics for biologists contains articles on many of the points above.

Software and code

Policy information about availability of computer code

Data collection	No software used.
Data analysis	RStudio v1.0.153; MACS v2.1.1; Integrated Genome Browser(9.0.1); All in-house scripts reported in the methods section are available in Github (https://github.com/sethiyap/FungalSporeAnalysis, https://github.com/zqmiao-mzq/closest_gene_calling/blob/master/zqWinSGR-v4.pl and https://github.com/zqmiao-mzq/closest_gene_calling/blob/master/closest_gene_calling_v10.pl); Online Bioinformatics analysis platform FungiExpressZ (https://cparsania.shinyapps.io/FungiExpresZ/); GraphPad Prism 7.0; MassLynx 4.1; ImageJ (1.5.0i); Image Lab v5.2.1; Bowtie2 (version: 2.2.9); hisat2 (version: 2.1.0).

For manuscripts utilizing custom algorithms or software that are central to the research but not yet described in published literature, software must be made available to editors and reviewers. We strongly encourage code deposition in a community repository (e.g. GitHub). See the Nature Research guidelines for submitting code & software for further information.

Data

Policy information about availability of data

All manuscripts must include a data availability statement. This statement should provide the following information, where applicable:

- Accession codes, unique identifiers, or web links for publicly available datasets
- A list of figures that have associated raw data
- A description of any restrictions on data availability

The following statement can be found in the manuscript:
"Next-Generation Sequencing data are available from NCBI SRA database under the accession number PRJNA602418 for RNAP II ChIPseq data, PRJNA602550 for TBP and TFIIB ChIPseq data, PRJNA602580 for RNAP I and RNAP III ChIPseq data, PRJNA602549 for histone modifications ChIPseq data and PRJNA607649 for RNAseq data. A list of figures that have associated raw data is given in Supplementary Table 10. Gene annotation and Gene Ontology information are obtained from AspGD (http://www.aspgd.org) and FungiDB (https://fungidb.org). Source data is available for Fig. 3, 4 and 5, Extended Data Fig. 4, 5, 7, 8 and 9 and Supplementary Fig. 3"

Field-specific reporting

Please select the one below that is the best fit for your research. If you are not sure, read the appropriate sections before making your selection.

☒ Life sciences ☐ Behavioural & social sciences ☐ Ecological, evolutionary & environmental sciences

For a reference copy of the document with all sections, see nature.com/documents/nr-reporting-summary-flat.pdf

Life sciences study design

All studies must disclose on these points even when the disclosure is negative.

Sample size	No prior assumptions were made regarding effect sizes. Three related fungal species (A. nidulans, A. fumigatus and T. marneffei) were chosen because one (A. nidulans) is a model organism with rich prior knowledge about conidia development while the other two species are human pathogens with medical significance. The number of spores to use in each experiment depends on the requirement of starting materials. For example, ~10^9 conidia provide enough total RNA for downstream analysis (e.g. RT-PCR and RNAseq). For liquid culture of mycelia, 100 ml culture was used because the resultant mycelial mass is sufficient for all experiments described in the work.
Data exclusions	No data was excluded from analysis.
Replication	For Western Blot, qPCR, conidial viability, conidia numbers, conidial ATP levels, growth assay by plate test, germination kinetics and virulence assay, the results presented are from at least three independent biological replicates as indicated in the corresponding figure legends. For experiments involving Next-Generation Sequencing, the results presented come from two highly correlated (i.e., reproducible) independent biological replicates (i.e., not technical replicates). Pearson's correlation coefficient was used to determine reproducibility between independent biological replicates of Next-Generation Sequencing data.
Randomization	Not relevant since samples were not allocated to experimental groups.
Blinding	Not relevant since samples were not allocated to experimental groups.

Reporting for specific materials, systems and methods

We require information from authors about some types of materials, experimental systems and methods used in many studies. Here, indicate whether each material, system or method listed is relevant to your study. If you are not sure if a list item applies to your research, read the appropriate section before selecting a response.

Materials & experimental systems

n/a	Involved in the study
☐	☒ Antibodies
☒	☐ Eukaryotic cell lines
☒	☐ Palaeontology and archaeology
☐	☒ Animals and other organisms
☒	☐ Human research participants
☒	☐ Clinical data
☒	☐ Dual use research of concern

Methods

n/a	Involved in the study
☐	☒ ChIP-seq
☒	☐ Flow cytometry
☒	☐ MRI-based neuroimaging

Antibodies

Antibodies used	Information about the antibodies used in ChIP experiments (e.g. catalogue number and dilution used) is provided in Supplementary

Antibodies used

Table 8.
Anti-Histone H3 antibody (H3), cat. ab1791, Abcam, 2ul used for ChIP; 1:5000 dilution for Western blotting;
Anti-acetyl-Histone H3 Antibody (H3Ac), cat. 06-599, Merck Millipore, 2ul used for ChIP;
Anti-Histone H3 (tri methyl K4) antibody (H3K4me3), cat. ab8580, Abcam, 2ul used for ChIP;
Anti-Histone H3 (tri methyl K36) antibody (H3K36me3), cat. ab9050, Abcam, 2ul used for ChIP;
Anti-RNA polymerase II subunit B1 (phospho-CTD Ser-5) Antibody (clone 3E8), cat. 04-1572, Merck Milllipore, 2ul used for ChIP;
c-Myc Antibody (9E10), cat. sc-40, Santa Cruze Biotechnology, 10ul used for ChIP; 1:2000 dilution for Western blotting;
HA-antibody(F7), cat. sc-7392, Santa Cruze Biotechnology, 10ul used for ChIP; 1:2000 dilution for Western blotting;
Flag-antibody, cat. F3165, Sigma M2, 1:5000 dilution for Western blotting;
Hsp70 antibody, cat. sc-32239, Santa Cruze Biotechnology, 1:2000 dilution for Western blotting;
HRP-conjugated anti-rabbit antibody, cat. AP132P, Merck Millipore, 1:5000 dilution for Western blotting;
HRP-conjugated anti-mouse antibody, cat. AP124P, Merck Millipore, 1:5000 dilution for Western blotting.

Validation

1. All antibodies used for ChIPseq (including anti-HA, anti-Myc, anti-Flag) are commonly used in the chromatin and transcription fields, and have been shown to have reactivity in diverse organisms including fungi and humans by the company supplier (Santa Cruze or Sigma). These antibodies were validated in our pull down assays by RT-PCR and western blot analysis on A. nidulans total protein extract. Those antibodies have been shown to work in diverse organisms by many literatures.

- References for [HA-antibody(F7)] usage in Aspergillus western Blot:
(Komachi et al., 2013); gfsA encodes a novel galactofuranosyltransferase involved in biosynthesis of galactofuranose antigen of O-glycan in Aspergillus nidulans and Aspergillus fumigatus.

- References for [c-Myc Antibody (9E10)] usage in Aspergillus western Blot:
(Levdansky, Kashi, Sharon, Shadkchan, & Osherov, 2010); The Aspergillus fumigatus cspA gene encoding a repeat-rich cell wall protein is important for normal conidial cell wall architecture and interaction with host cells.

- References for [Flag-antibody, cat. F3165, Sigma M2] usage in Aspergillus western Blot:
(Ni & Yu, 2007); A novel regulator couples sporogenesis and trehalose biogenesis in Aspergillus nidulans.
(Lee et al., 2016); Negative regulation and developmental competence in Aspergillus.

-References for [Flag-antibody, cat. F3165, Sigma M2] usage in yeast ChIPseq:
(Su, Lu, & Liu, 2016); N-acetylglucosamine sensing by a GCN5-related N-acetyltransferase induces transcription via chromatin histone acetylation in fungi.

2. anti-Pol II (3e8) antibody has been shown to work in diverse organisms by many literatures, and was validated in our pull down assays by RT-PCR and western blot analysis on A. nidulans total protein extract.

- References for [phospho-CTD Ser-5 Antibody (clone 3E8), cat. 04-1572, Merck Milllipore] usage in yeast ChIPseq:
(Vassiliadis, Wong, Andrianopoulos, & Monahan, 2019); A genome-wide analysis of carbon catabolite repression in Schizosaccharomyces pombe.

3. The antibodies used for and Histone ChIPseq (H3; H3K4me3; H3K36me3 and H3Ac) are commonly used in the chromatin and transcription fields. These antibodies have been shown to have reactivity in diverse organisms including fungi and humans by the company supplier (Abcam or Millipore). All these antibodies were validated in our pull down assays by RT-PCR.

- References for H3; H3K4me3; H3K36me3 and H3Ac antibodies usage in Aspergillus nidulans ChIPseq experiment:
(Gacek-Matthews et al., 2016); KdmB, a Jumonji histone H3 demethylase, regulates genome-wide H3K4 trimethylation and is required for normal induction of secondary metabolism in Aspergillus nidulans.

- References for [Anti-Histone H3 antibody (H3), cat. ab1791, Abcam] usage in yeast ChIPseq experiment:
(Su, Lu, & Liu, 2016); N-acetylglucosamine sensing by a GCN5-related N-acetyltransferase induces transcription via chromatin histone acetylation in fungi.

- References for [Anti-acetyl-Histone H3 Antibody (H3Ac), cat. 06-599, Merck Millipore] usage in yeast western Blot experiment:
(Friis et al., 2009); A glycolytic burst drives glucose induction of global histone acetylation by picNuA4 and SAGA.

- References for [Anti-Histone H3 (tri methyl K4) antibody (H3K4me3), cat. ab8580, Abcam] usage in fungi ChIPseq and Western Blot experiment:
(Lai et al., 2020); Coordinated regulation of infection-related morphogenesis by the KMT2-Cre1-Hyd4 regulatory pathway to facilitate fungal infection.

- References for [Anti-Histone H3 (tri methyl K36) antibody (H3K36me3), cat. ab9050, Abcam] usage in yeast western Blot experiment:
(Kaczmarek Michaels, Mohd Mostafa, Ruiz Capella, & Moore, 2020); Regulation of alternative polyadenylation in the yeast Saccharomyces cerevisiae by histone H3K4 and H3K36 methyltransferases.

4. The anti-Hsp70 antibody was validated by western blot analysis on our A. nidulans total protein extract, and the size of the observed protein band is consistent with the expected size for Hsp70.

- References for [Hsp70 antibody, cat. sc-32239, Santa Cruze Biotechnology] usage in human western Blot experiment:
(Wu et al., 2019); Identification of the PTEN-ARID4B-PI3K pathway reveals the dependency on ARID4B by PTEN-deficient prostate cancer.

Animals and other organisms

Policy information about studies involving animals; ARRIVE guidelines recommended for reporting animal research

Laboratory animals	Galleria mellonella larvae weighing about 0.3 g were used. They were obtained from a commercial source.
Wild animals	This study did not involve wild animals.
Field-collected samples	This study did not involve samples collected from the field.
Ethics oversight	No ethical approval or guidance was required.

Note that full information on the approval of the study protocol must also be provided in the manuscript.

ChIP-seq

Data deposition

☒ Confirm that both raw and final processed data have been deposited in a public database such as GEO.

☒ Confirm that you have deposited or provided access to graph files (e.g. BED files) for the called peaks.

Data access links
May remain private before publication.

https://www.ncbi.nlm.nih.gov/sra/?term=PRJNA602418
https://www.ncbi.nlm.nih.gov/sra/?term=PRJNA602550
https://www.ncbi.nlm.nih.gov/sra/?term=PRJNA602580
https://www.ncbi.nlm.nih.gov/sra/?term=PRJNA602549
https://www.ncbi.nlm.nih.gov/sra/?term=PRJNA607649

Files in database submission

af293_17d_spore_polII_repeat1_CGAACTGTG_CL_ChIPmix22_R1.fastq.gz
af293_17d_spore_polII_repeat2_CAGGAGGCGT_ChIPMix71_R1.fastq.gz
af293_3d_spore_polII_repeat1_ACGTAGCTC_CL_ChIPmix22_R1.fastq.gz
af293_3d_spore_polII_repeat2_AACCGTGTT_ChIPMix44_R1.fastq.gz
af293_ANM_spore_polII_repeat1_CCATACAC_CL_ChIPmix25_R1.fastq.gz
af293_ANM_spore_polII_repeat2_ATATAGGAT_ChIPMix75_R1.fastq
af293_input_3d_spore_TGAGAGTG_CL1019Mix_R1.fastq.gz
af293_Kcl_spore_polII_repeat1_GTCTACAT_CL_ChIPmix25_R1.fastq.gz
af293_KCl_spore_polII_repeat2_AGGTCAGTT_ChIPMix75_R1.fastq
af293_NaCl_spore_polII_repeat1_CGCATTAA_CL_ChIPmix25_R1.fastq.gz
af293_NaCl_spore_polII_repeat2_AACCGTGTT_ChIPMix75_R1.fastq
af293_Zinc-_spore_polII_repeat1_GAGTTAAC_CL_ChIPmix25_R1.fastq.gz
af293_zinc-_spore_polII_repeat2_CTCTGTCTT_ChIPMix75_R1.fastq
An_17d_spore_polII_repeat1_ChIPMix10_TCCAGCCTC_R1.fastq.gz
AN_17d_spore_polII_repeat2_ATCGCCAGCT_ChIPMix71_R1.fastq.gz
An_3d_spore_37°C_4h_polII_repeat1_GCCAAT_CL_ChIPmix25_R1.fastq.gz
An_3d_spore_37°C_4h_polII_repeat2_CCATACACT_ChIPMix75_R1.fastq
An_3d_spore_4°C_4h_polII_repeat1_CAGATC_CL_ChIPmix25_R1.fastq.gz
An_3d_spore_4°C_4h_polII_repeat2_CGCATTAAT_ChIPMix75_R1.fastq
An_3d_spore_42°C_4h_polII_repeat1_ACTTGA_CL_ChIPmix25_R1.fastq.gz
An_3d_spore_42°C_4h_polII_repeat2_GTCTACATT_ChIPMix75_R1.fastq
An_3d_spore_polII_repeat1_GTTGTCCCA_CL_ChIPmix22_R1.fastq.gz
An_3d_spore_polII_repeat2_TGATCCGA_CL_ChIPmix22_R1.fastq.gz
An_6d_spore_polII_repeat1_ChIPmix04_TAGCTT_R1.fastq.gz
An_6d_spore_polII_repeat2_CGATGT_CL_ChIPmix25_R1.fastq.gz
An_ANM_spore_polII_repeat1_ATATAGGA_CL_ChIPmix25_R1.fastq.gz
An_ANM_spore_polII_repeat2_ChIPMix68_R1.fastq.gz
An_hyphae_polII_repeat1_CATTCCAAG_CL_ChIPmix22_R1.fastq.gz
An_hyphae_polII_repeat2_CGGACGTGG_ChIPmix11.fastq.gz
An_input_3d_spore_CACAGTTGG_CL1019Mix_R1.fastq.gz
An_KCl_spore_polII_repeat1_AGGTCAGT_CL_ChIPmix25_R1.fastq.gz
An_KCl_spore_polII_repeat2_ACTTGAT_ChIPMix68_R1.fastq.gz
An_NaCl_spore_polII_repeat1_AACCGTGT_CL_ChIPmix25_R1.fastq.gz
An_NaCl_spore_polII_repeat2_CAGATCT_ChIPMix68_R1.fastq.gz
An_spore_H3_repeat1_AGAACACC_CL1019Mix_R1.fastq.gz
An_spore_H3_repeat2_CATTCCAAGT_ChIPMix71_R1.fastq.gz
An_spore_H3AC_repeat1_ATCCTATTC_CL_ChIPmix22_R1.fastq.gz
An_spore_H3Ac_repeat2_CGCATTAA_mix33_fang_R1.fastq.gz
An_spore_H3K36me3_repeat1_GCGTTTCGA_CL_ChIPmix22_R1.fastq.gz
An_spore_H3K36me3_repeat2_ATATAGGA_mix33_fang_R1.fastq.gz
An_spore_H3K4me3_repeat1_CGGACGTGG_CL_ChIPmix22_R1.fastq.gz
An_spore_H3K4me3_repeat2_TAGCTT_mix33_fang_R1.fastq.gz
An_TBP_MYC_hyphae_repeat1_GCAGCCTC_CL_ChIPmix22_R1.fastq
An_TBP_MYC_hyphae_repeat2_AACACCTAC_CL_ChIPmix22_R1.fastq
An_TBP_MYC_spore_repeat1_GATCAG_CL_ChIPmix22_R1.fastq.gz

An_TBP_MYC_spore_repeat2_ATATAGGA_CL_ChIPmix22_R1.fastq.gz
An_TFIIB_MYC_hyphae_repeat1_TCGCGTAC_CL_ChIPmix22_R1.fastq.gz
An_TFIIB_MYC_hyphae_repeat2_CCTTTACAG_CL_ChIPmix22_R1.fastq.gz
An_TFIIB_MYC_spore_repeat1_TAGCTT_CL_ChIPmix22_R1.fastq.gz
An_TFIIB_MYC_spore_repeat2_AACCGTGT_CL_ChIPmix22_R1.fastq.gz
An_Zinc-_spore_polII_repeat1_CTCTGTCT_CL_ChIPmix25_R1.fastq.gz
An_Zinc-_spore_polII_repeat2_ATCACGT_ChIPMix68_R1.fastq.gz
AtfA_MYC_spore_repeat1_TATCTCCGT_ChIPMix57_R1.fastq.gz
AtfA_MYC_spore_repeat2_CGATGTT_ChIPMix71_R1.fastq.gz
RPA43_HA_AN9102_hyphae_repeat1_GGCAGACGAT_ChIPMix49_R1.fastq.gz
RPA43_HA_AN9102_hyphae_repeat2_CTTGTAT_ChIPMix71_R1.fastq.gz
RPA43_HA_AN9102_spore_repeat1_TAGCTAGTAT_ChIPMix49_R1.fastq.gz
RPA43_HA_AN9102_spore_repeat2_TTAGGCT_ChIPMix71_R1.fastq.gz
RPC11_MYC_AN4219_spore_repeat1_CGAACTGTGT_ChIPMix49_R1.fastq.gz
RPC11_MYC_AN4219_spore_repeat2_GATCAGT_ChIPMix71_R1.fastq.gz
RPC40_HA_AN2415_hyphae_repeat1_GTGACTACAT_ChIPMix49_R1.fastq.gz
RPC40_HA_AN2415_hyphae_repeat2_ATATAGGAT_ChIPMix71_R1.fastq.gz
RPC40_HA_AN2415_spore_repeat1_GCAAGTAGAT_ChIPMix49_R1.fastq.gz
RPC40_HA_AN2415_spore_repeat2_TGACCAT_ChIPMix71_R1.fastq.gz
RPO31_HA_AN10316_hyphae_repeat1_TGAGAGTGT_ChIPMix49_R1.fastq.gz
RPO31_HA_AN10316_hyphae_repeat2_CTCTGTCTT_ChIPMix71_R1.fastq.gz
RPO31_HA_AN10316_spore_repeat1_TGATCCGAT_ChIPMix49_R1.fastq.gz
RPO31_HA_AN10316_spore_repeat2_ACTTGAT_ChIPMix71_R1.fastq.gz
TFIIIB_HA_AN3116_hyphae_repeat1_TTCTGATGT_ChIPMix49_R1.fastq.gz
TFIIIB_HA_AN3116_hyphae_repeat2_AGGTCAGTT_ChIPMix71_R1.fastq.gz
TFIIIB_HA_AN3116_spore_repeat1_GTGGGATAT_ChIPMix49_R1.fastq.gz
TFIIIB_HA_AN3116_spore_repeat2_CAGATCT_ChIPMix71_R1.fastq.gz
TFIIIC_HA_AN7997_spore_repeat1_ACGTAGCTCT_ChIPMix49_R1.fastq.gz
TFIIIC_HA_AN7997_spore_repeat2_GCCAATT_ChIPMix71_R1.fastq.gz
Tm_input_spore_GTGACTACA_CL1019Mix_R1.fastq.gz
Tm_spore_polII_repeat1_GGCTAC_CL_ChIPmix25_R1.fastq.gz
Tm_spore_polII_repeat2_TGACGCAT_CL_ChIPmix22_R1.fastq.gz
WetA_MYC_spore_repeat1_TATCTCCGT_ChIPMix49_R1.fastq.gz
WetA_MYC_spore_repeat2_ATCACGT_ChIPMix71_R1.fastq.gz
Outdoor_spore_repeat1_15_18_Aug_CTAGATTCGT_ChIPMix92_S57_L002_R1_001.fastq.gz
Outdoor_spore_repeat1_15_18_Aug_CTAGATTCGT_ChIPMix92_S57_L001_R1_001.fastq.gz
Outdoor_spore_repeat2_15_18_Aug_GAACGCTGAT_ChIPMix92_S58_L002_R1_001.fastq.gz
Outdoor_spore_repeat2_15_18_Aug_GAACGCTGAT_ChIPMix92_S58_L001_R1_001.fastq.gz
Outdoor_spore_repeat1_7_10_Nov_ACTTGAT_ChIPMix91_R1_002.fastq.gz
Outdoor_spore_repeat1_7_10_Nov_ACTTGAT_ChIPMix91_R1_001.fastq.gz
Outdoor_spore_repeat2_7_10_Nov_GATCAGT_ChIPMix91_R1_002.fastq.gz
Outdoor_spore_repeat2_7_10_Nov_GATCAGT_ChIPMix91_R1_001.fastq.gz
Outdoor_spore_repeat1_2_5_Sep_ATCACGT_ChIPMix91_R1_002.fastq.gz
Outdoor_spore_repeat1_2_5_Sep_ATCACGT_ChIPMix91_R1_001.fastq.gz
Outdoor_spore_repeat2_2_5_Sep_CGATGTT_ChIPMix91_R1_002.fastq.gz
Outdoor_spore_repeat2_2_5_Sep_CGATGTT_ChIPMix91_R1_001.fastq.gz

Genome browser session
(e.g. UCSC)

No longer applicatable

Methodology

Replicates

All ChIPseq experiments were performed in two independent biological repeats.

Sequencing depth

A summary of the number of mapped reads and read length for each dataset is provided in Supplementary Table 11.

Antibodies

Information about the antibodies used (e.g. catalogue number and dilution used) is provided in Supplementary Table 8. The following antibodies are commercially available and commonly used in ChIP experiments by the chromatin and transcription fields, and have been shown to work in diverse organisms including fungi and humans. There are extensive references showing their validity, and they can be provided upon request.
Anti-Histone H3 antibody (H3), cat. ab1791, Abcam, 2ul used;
Anti-acetyl-Histone H3 Antibody (H3Ac), cat. 06-599, Merck Millipore, 2ul used;
Anti-Histone H3 (tri methyl K4) antibody (H3K4me3), cat. ab8580, Abcam, 2ul used;
Anti-Histone H3 (tri methyl K36) antibody (H3K36me3), cat. ab9050, Abcam 2ul used;
Anti-RNA polymerase II subunit B1 (phospho-CTD Ser-5) Antibody (clone 3E8), cat. 04-1572, Merck Milllipore, 2ul used;
c-Myc Antibody (9E10), cat. sc-40, Santa Cruze Biotechnology, 10ul used;
HA-antibody(F7), cat. sc-7392, Santa Cruze Biotechnology, 10ul used.

Peak calling parameters

Bowtie2 was used for mapping using the following parameters:
bowtie2 -p 2 --trim5 8 --local -x <genome_reference PATH> -U <fastq.gz PATH> | samtools view -bS - | samtools sort -O bam -o <bam PATH>
samtools index <bam PATH>
samtools flagstat /.bam > alignment.stats
mappedReads=`grep -P ' 0 mapped \(' alignment.stats | grep -P -o '^\d+'`
scale=`perl -e "printf('%.3f', 1000000/$mappedReads)"`

MACS2 was used for peak calling:
macs2 callpeak --nomodel -t ${file} -f BAM -g 30517219 -n ${file}_macs2

ChIPseq signal was calculated using an in-house script available from Github (https://github.com/zqmiao-mzq/closest_gene_calling/blob/master/zqWinSGR-v4.pl and https://github.com/zqmiao-mzq/closest_gene_calling/blob/master/closest_gene_calling_v10.pl)

Data quality

All biological replicates have correlation values equal to or greater than 0.8 with a median correlation of 0.9 across all experiments, except for three experiments. They are ChIPseq against Rpa43 (0.77) and Tfc1 (0.7) in A. nidulans spores, and RNAPII in 17-day A. fumigatus spores (0.71). For Rpa43 and Tfc1 (a subunit of RNAP I and RNAP III, respectively), the replicates are qualitatively similar and showing the same results reported. Moreover, we performed ChIPseq against multiple different subunits for the RNAP I and III transcription complexes as independent confirmation. Those different subunits had consistent results and can be considered as "independent repeats". Therefore, the slightly lower correlation for these two pairs of data did not affect the conclusion made. For RNAP II 17-day A. fumigatus spores, the main result (e.g. different transcription profiles for 3 and 17 day old spores) was observed in both repeat datasets at the genome-browser level and consistent with the result shown for A. nidulans, which was the main result used for drawing the conclusion. Therefore, the slightly lower correlation for this pair of datasets did not affect the conclusion.

Software

RStudio v1.0.153;
MACS v2.1.1;
Integrated Genome Browser(9.0.1);
In-house scripts (https://github.com/sethiyap/FungalSporeAnalysis);
In-house scripts (https://github.com/zqmiao-mzq/closest_gene_calling/blob/master/zqWinSGR-v4.pl and https://github.com/zqmiao-mzq/closest_gene_calling/blob/master/closest_gene_calling_v10.pl);
Online Bioinformatics analysis platform FungiExpressZ (https://cparsania.shinyapps.io/FungiExpresZ/).